



Highlights from 10 years observations with CALET on the International Space Station

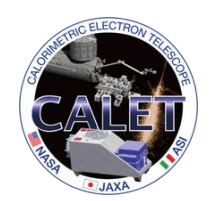


CALET

Kazuyoshi Kobayashi
Waseda university
for CALET collaboration



TAUP@Xichang, Sichuan, China, Aug. 24-30, 2025



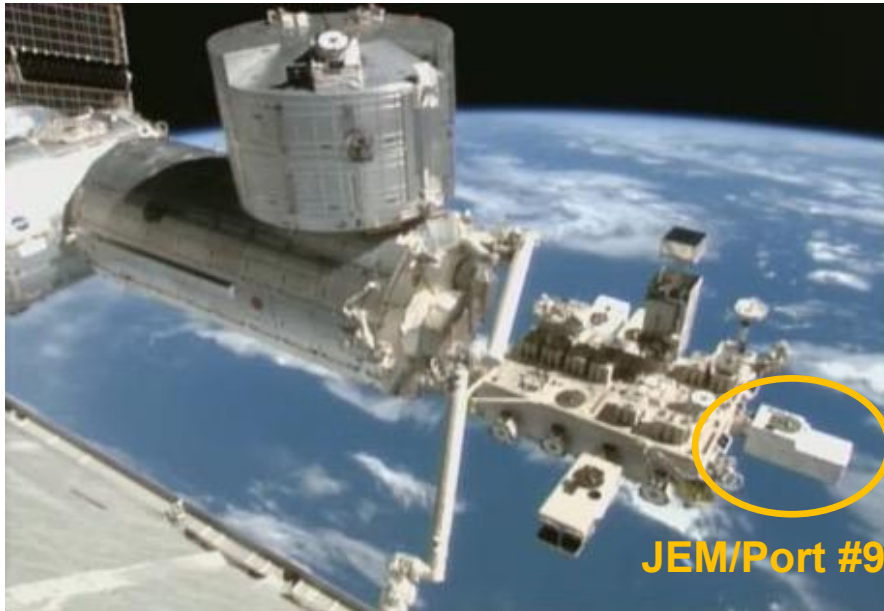
CALET Payload



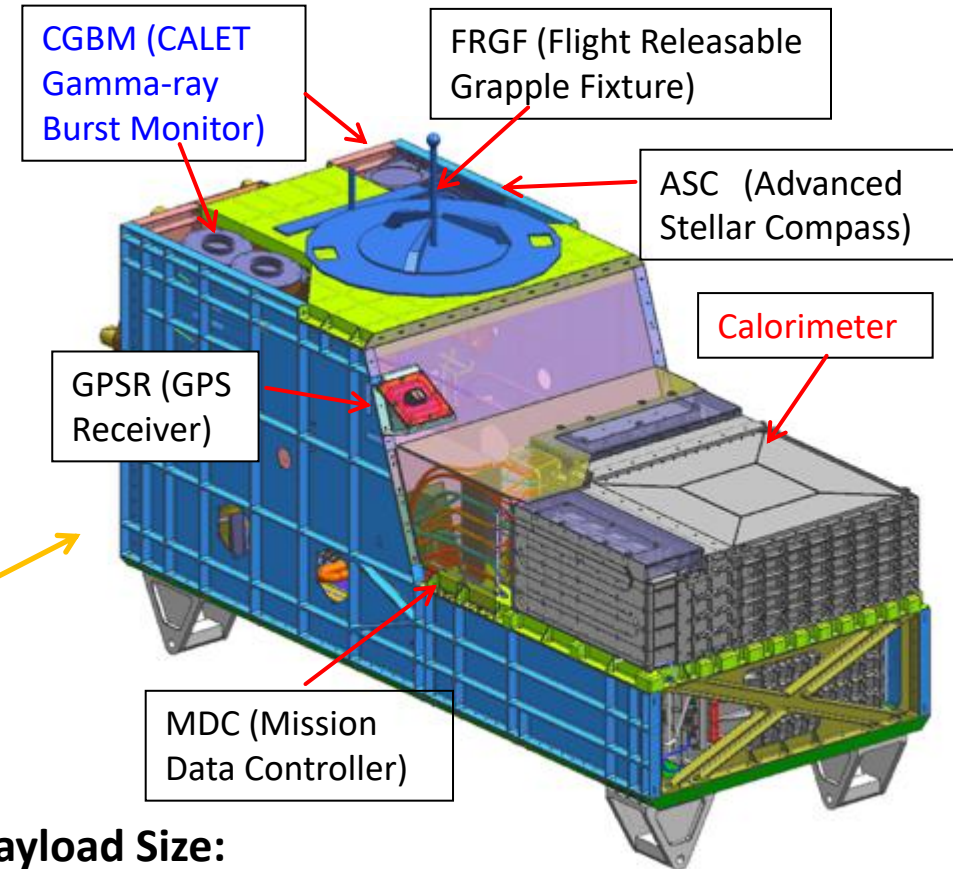
Kounotori (HTV) 5



- Launched on Aug. 19th, 2015 by the Japanese H2-B rocket.
- Emplaced on JEM-EF port #9 on Aug. 25th, 2015



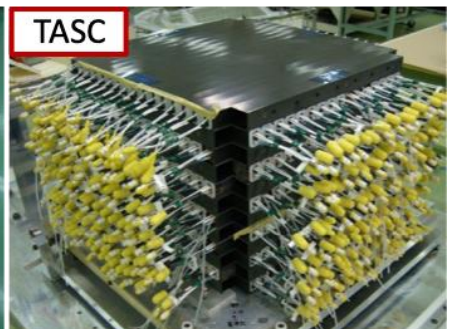
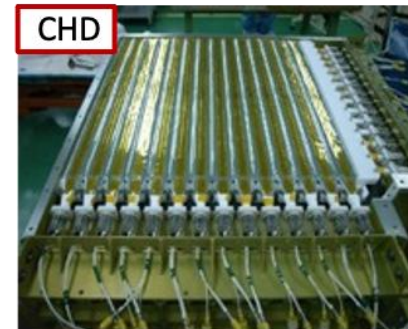
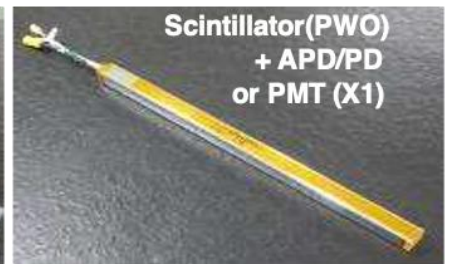
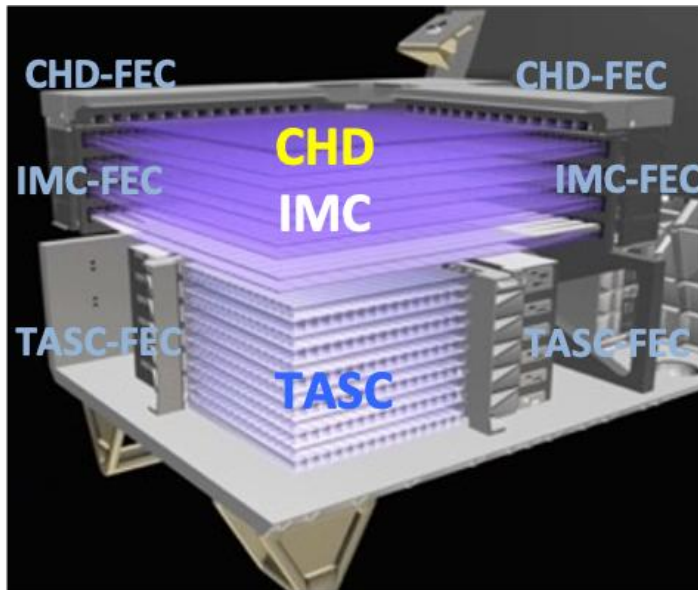
JEM/Port #9



- Mass: 612.8 kg
- JEM Standard Payload Size:
1850mm(L) × 800mm(W) × 1000mm(H)
- Power Consumption: 507 W (max)
- Telemetry:
Medium 600 kbps (6.5GB/day) / Low 50 kbps



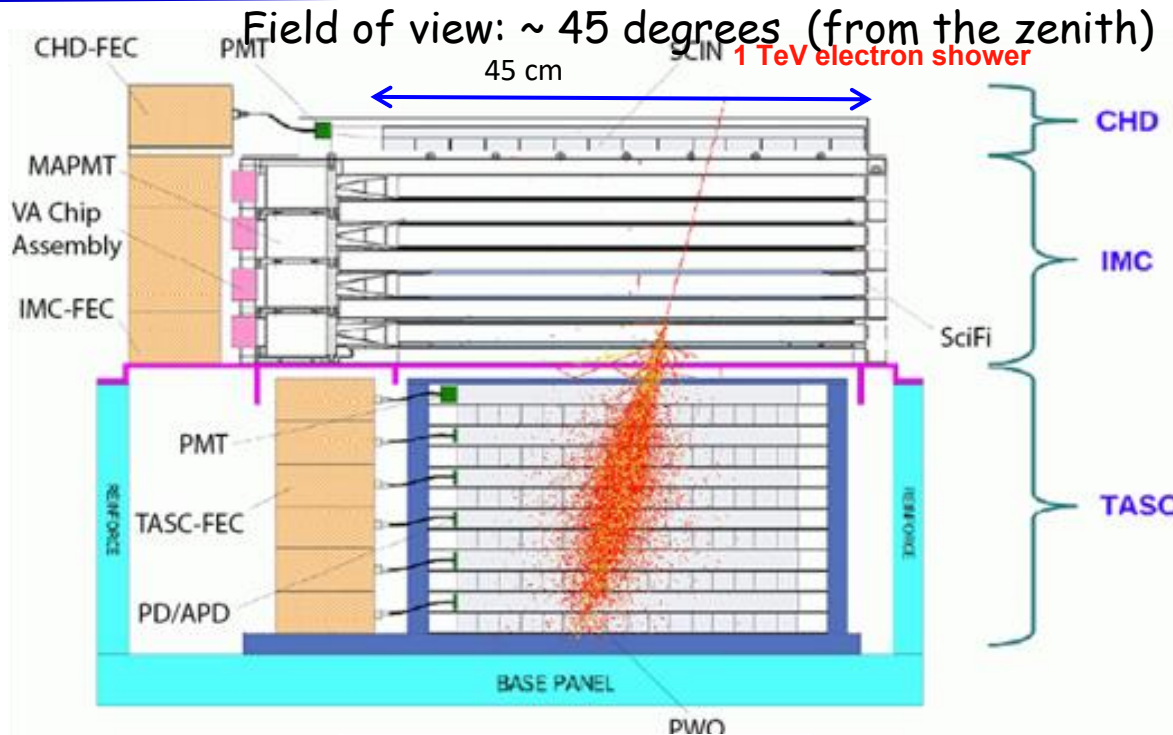
CALET Detector: Calorimeter



| | CHD (Charge Detector) | IMC (Imaging Calorimeter) | TASC (Total Absorption Calorimeter) |
|------------------------|---|--|---|
| Measure | Charge ($Z=1-40$) | Tracking , Particle ID | Energy, e/p Separation |
| Geometry (Material) | Plastic Scintillator 14 paddles x 2 layers (X,Y): 28 paddles Paddle Size: 32 x 10 x 450 mm ³ | 448 Scifi x 16 layers (X,Y) : 7168 Scifi 7 W layers ($3X_0$): $0.2X_0 \times 5 + 1X_0 \times 2$ Scifi size : 1 x 1 x 448 mm ³ | 16 PWO logs x 12 layers (x,y): 192 logs log size: 19 x 20 x 326 mm ³ Total Thickness : $27 X_0$, $\sim 1.2 \lambda_1$ |
| Readout | PMT+CSA | 64-anode PMT + ASIC (VA32-HDR) | APD/PD+CSA PMT+CSA (for Trigger)@top layer |



CALET Calorimeter and Capability



CHD – Charge Detector

- 2 layers x 14 plastic scintillating paddles
- single element charge ID from p to Fe and above ($Z = 40$)
- charge resolution $\sim 0.1\text{-}0.3 \text{ e}$

IMC – Imaging Calorimeter

- Scifi + Tungsten absorbers: $3 X_0$ at normal incidence
- $8 \times 2 \times 448$ plastic scintillating fibers (1mm) **readout individually**
- **Tracking** ($\sim 0.1^\circ$ angular resolution) + **Shower imaging**

TASC – Total Absorption Calorimeter $27 X_0$, $1.2 \lambda_I$

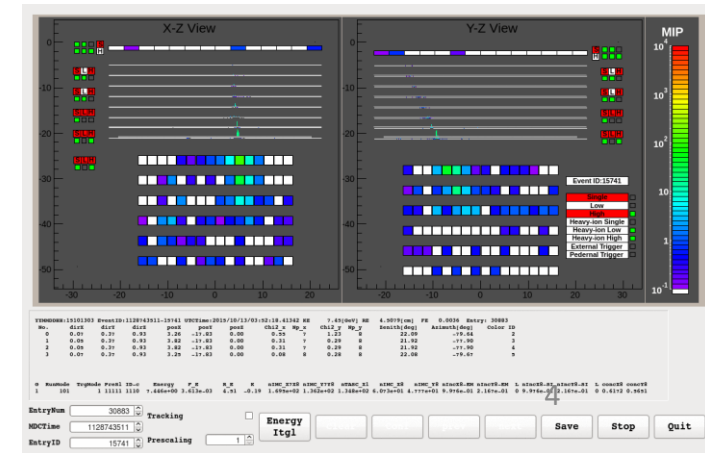
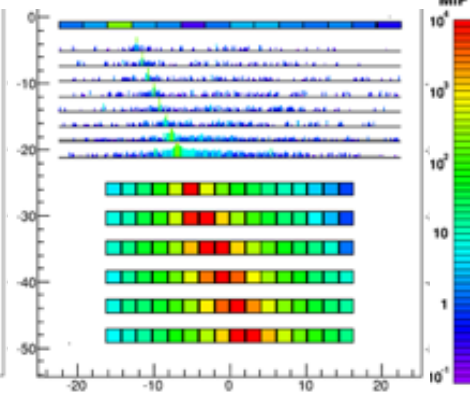
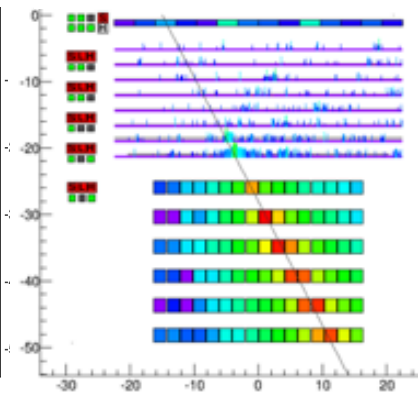
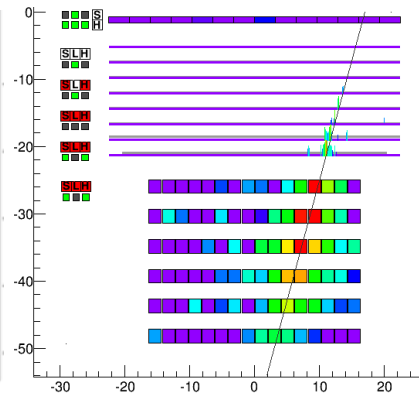
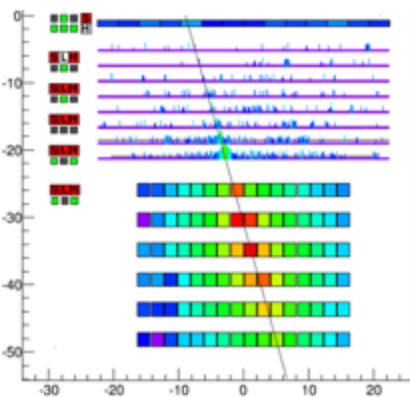
- $6 \times 2 \times 16$ lead tungstate (PbWO_4) logs
- **Energy resolution:** $\sim 2 \%$ ($>10\text{GeV}$) for e, γ $\sim 30\text{-}35\%$ for p, nuclei
- **e/p separation:** $\sim 10^{-5}$

Electron, $E=3.05 \text{ TeV}$

Gamma-ray, $E=44.3 \text{ GeV}$

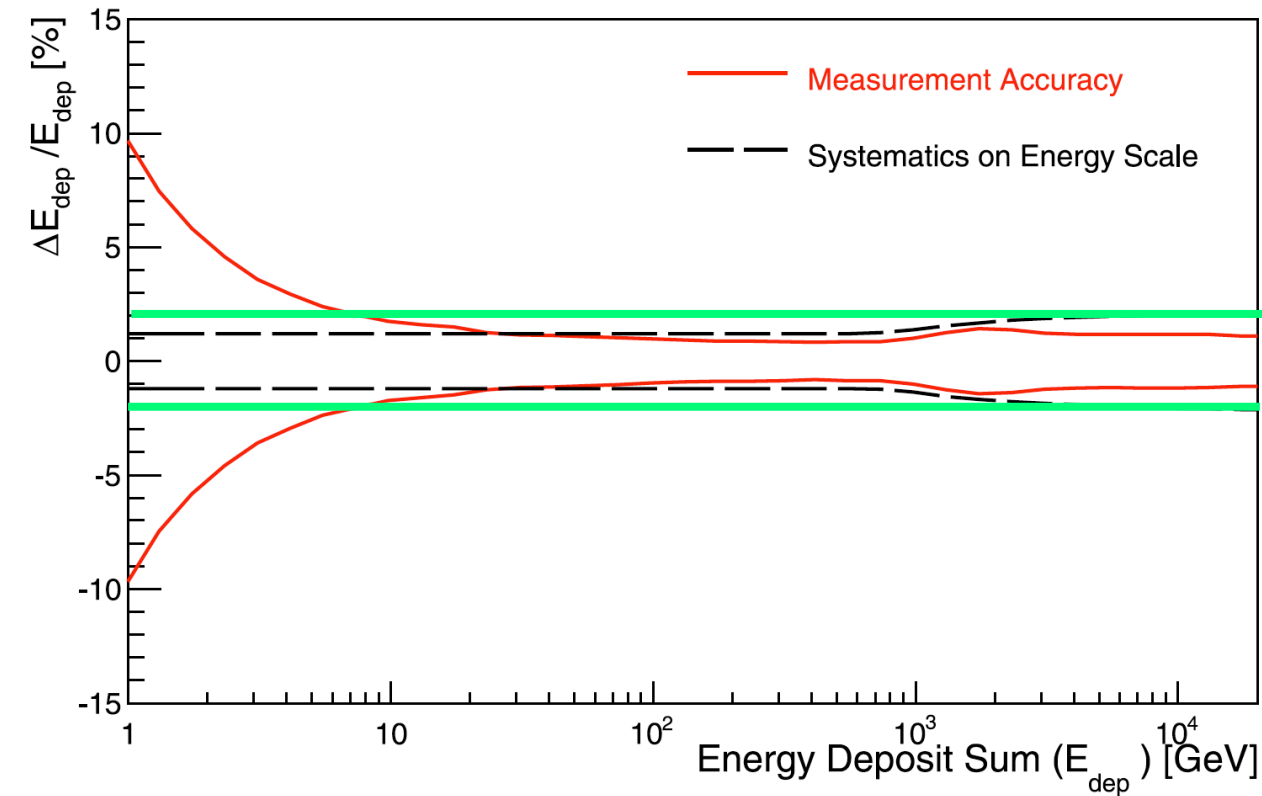
Proton, $E_{\text{TASC}}=2.89 \text{ TeV}$

Iron, $E_{\text{TASC}}=9.3 \text{ TeV}$

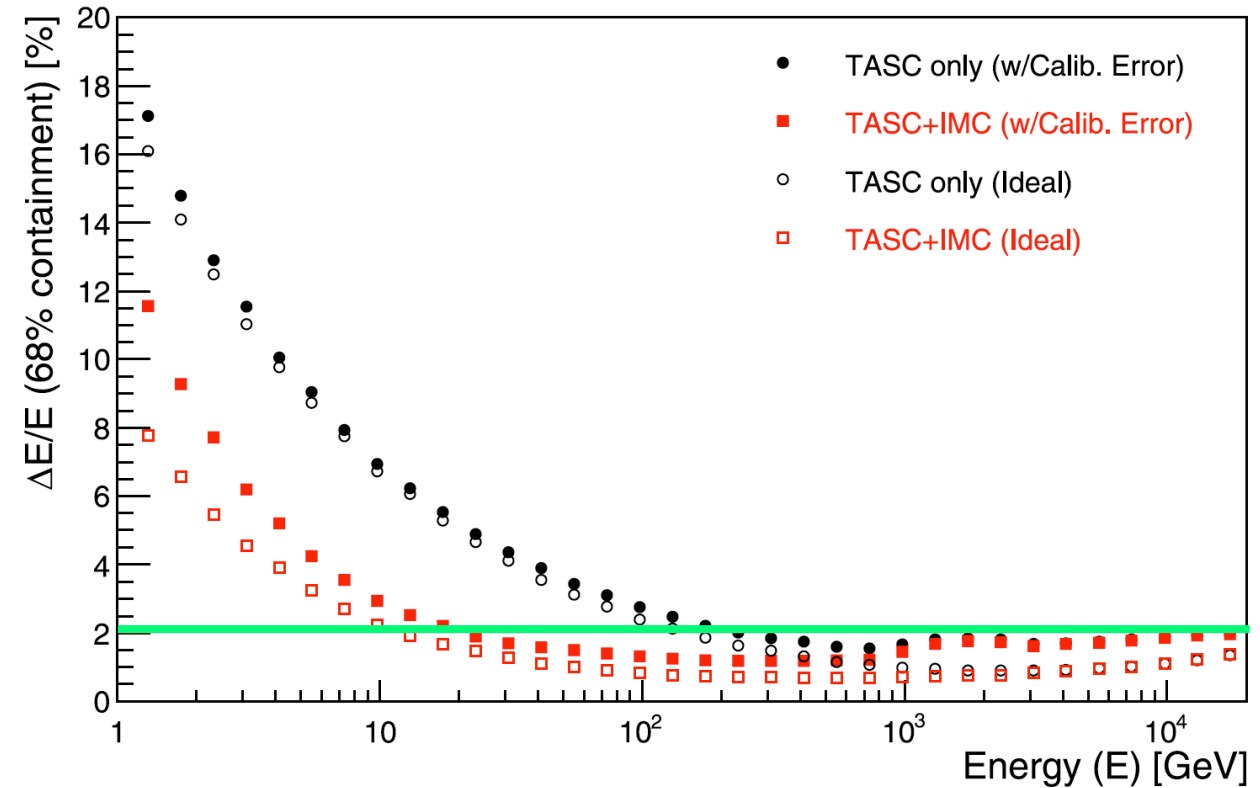


Energy Deposit Resolution in the Calorimeter

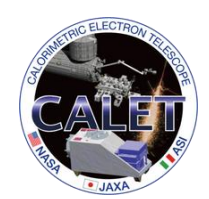
Asaoka et al. 2017, Astropart. Phys. 91, 1-10



Energy deposit resolution in the TASC is better than 2% above ~ 8 GeV



Reconstructed energy resolution is better than 2% for electrons above ~ 20 GeV



CALET Scientific Goal

Detector
performance

- **Geometrical Factor:**
1040 cm² sr for electrons, light nuclei
1000 cm² sr for gamma-rays
4000 cm²sr for ultra-heavy nuclei
- **ΔE/E:**
~2 % (>10GeV) for e , γ
~30-35% for protons, nuclei
- **e/p separation:** ~10⁵
- **Charge resolution:** 0.15-3 e (p-Fe)
- **Angular resolution:**
0.2° for gamma-rays > ~50 GeV

Scientific
objectives

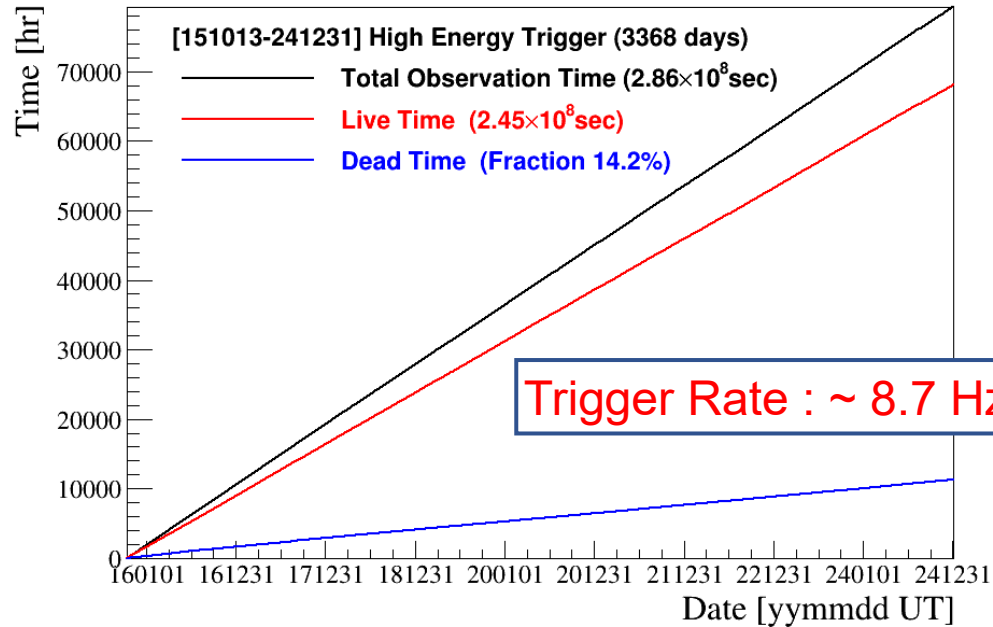
- ◆ **Electron observation in 1GeV-20TeV**
Design optimized for electron detection:
high energy resolution and large e/p separation power
+ electromagnetic shower containment
Search for Dark Matter and Nearby Sources
- ◆ **Observation of cosmic-rays in 10 GeV-1 PeV**
CR acceleration and propagation mechanism(s)
- ◆ **Detection of transient phenomena in space:**
 - Gamma-ray burst
 - GW e.m. counterparts
 - Solar modulation
 - Space weather

| Scientific Objectives | Observation Targets | Energy Range |
|----------------------------|---|--|
| CR Origin and Acceleration | Electron spectrum Individual spectra of elements from proton to Fe Ultra Heavy Ions (26<Z≤40) Gamma-rays (Diffuse + Point sources) | 1GeV - 20 TeV 10 GeV - 1000 TeV > 600 MeV/n 1 GeV - 1 TeV |
| Galactic CR Propagation | B/C and sub-Fe/Fe ratios | Up to some TeV/n |
| Nearby CR Sources | Electron spectrum | 100 GeV - 20 TeV |
| Dark Matter | Signatures in electron/gamma-ray spectra | 100 GeV - 20 TeV |
| Solar Physics | Electron flux (1GeV-10GeV) | < 10 GeV |
| Gamma-ray Transients | Gamma-rays and X-rays | 7 keV - 20 MeV |



CALET Observation on the ISS

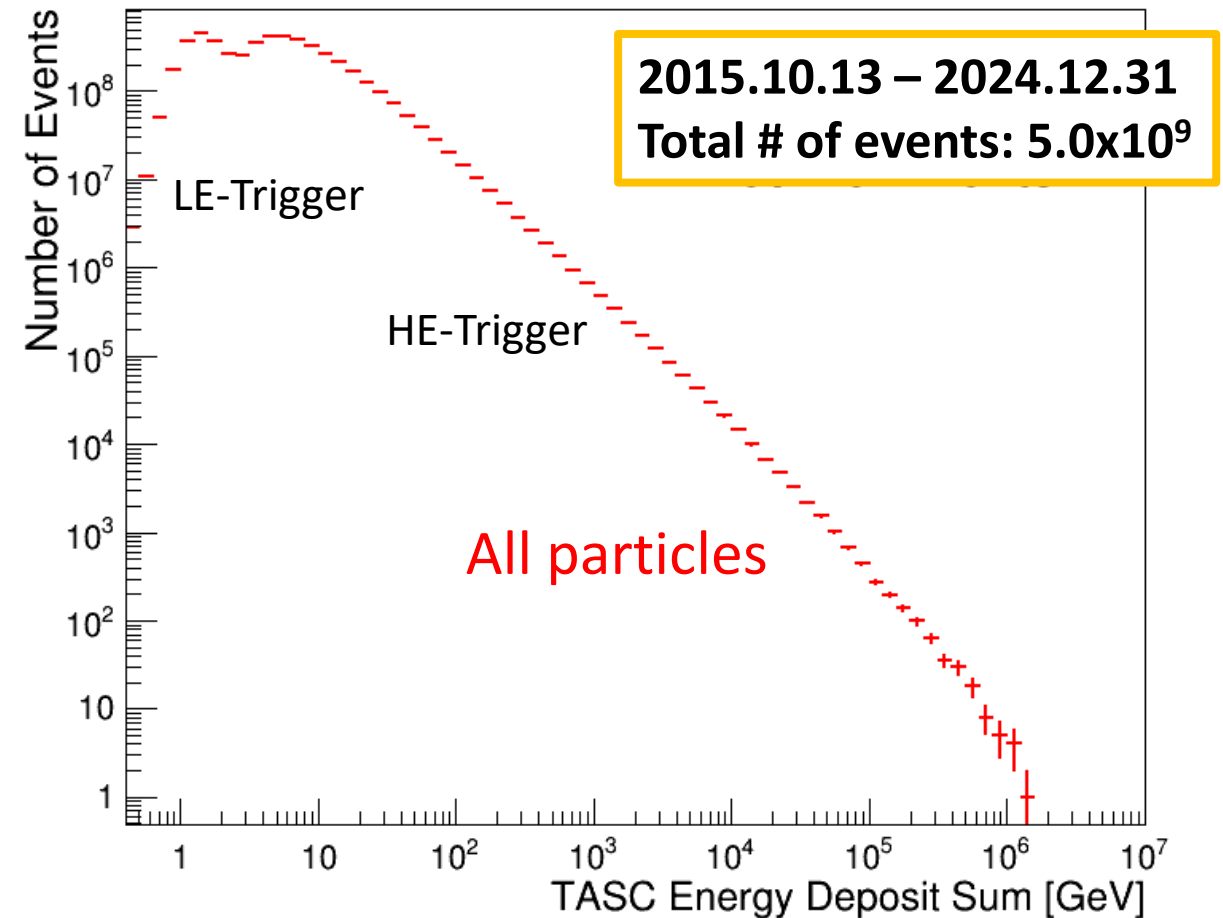
Accumulated observation time (live, dead)



High-energy trigger (> 10 GeV) statistics:

- Operational time: **3368 days** as of Dec. 31, 2024
- Live time fraction: **$> 85\%$**
- Exposure of HE trigger: **$\sim 300 \text{ m}^2 \text{ sr day}$**

Energy deposit (in TASC) spectrum: 1 GeV-1 PeV

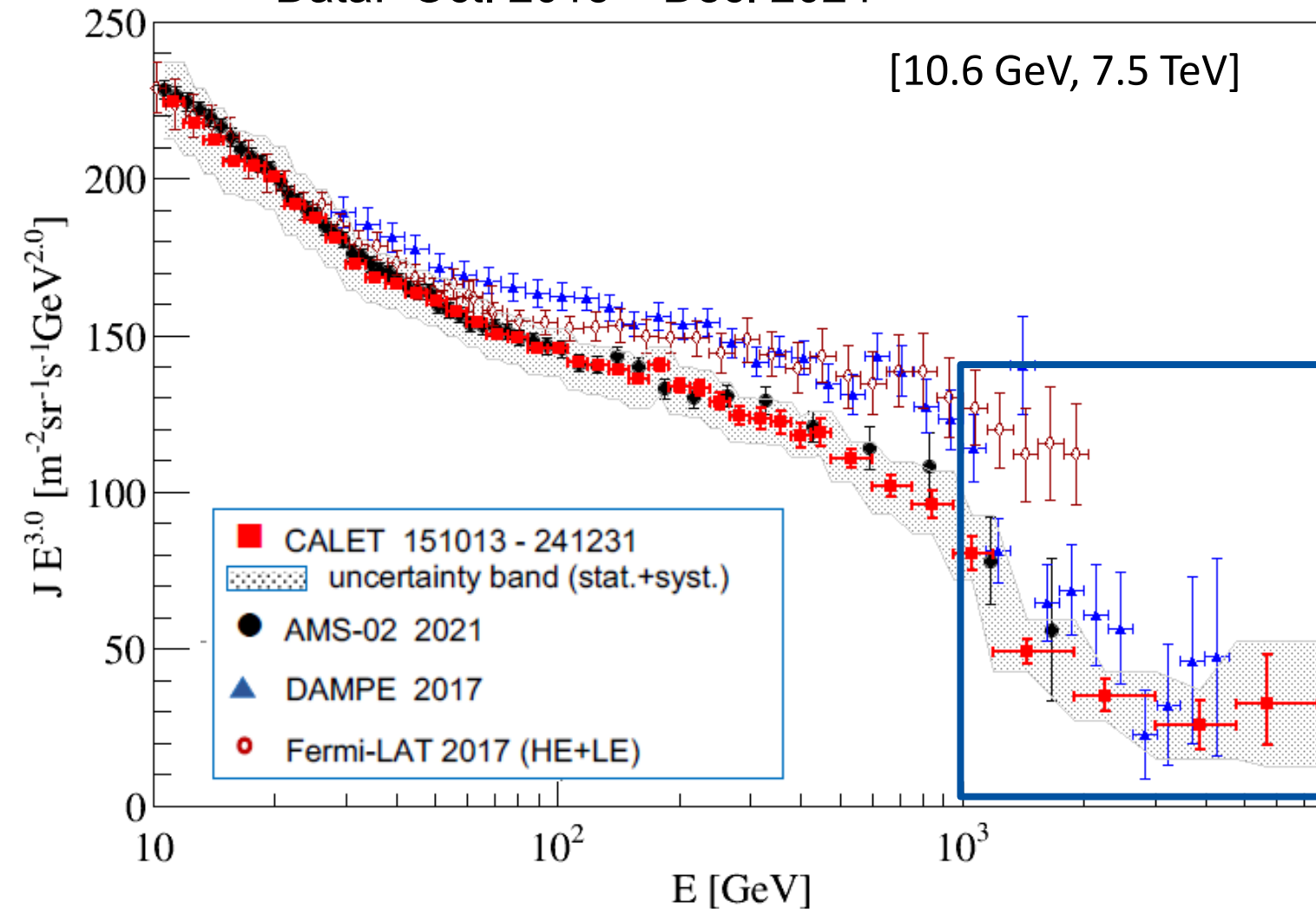




Cosmic-ray all-electron spectrum

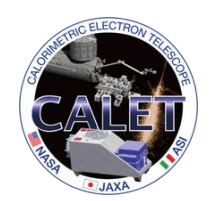
PRL 131, 191001 (2023)
ICRC2025 update

Data: Oct. 2015 – Dec. 2024



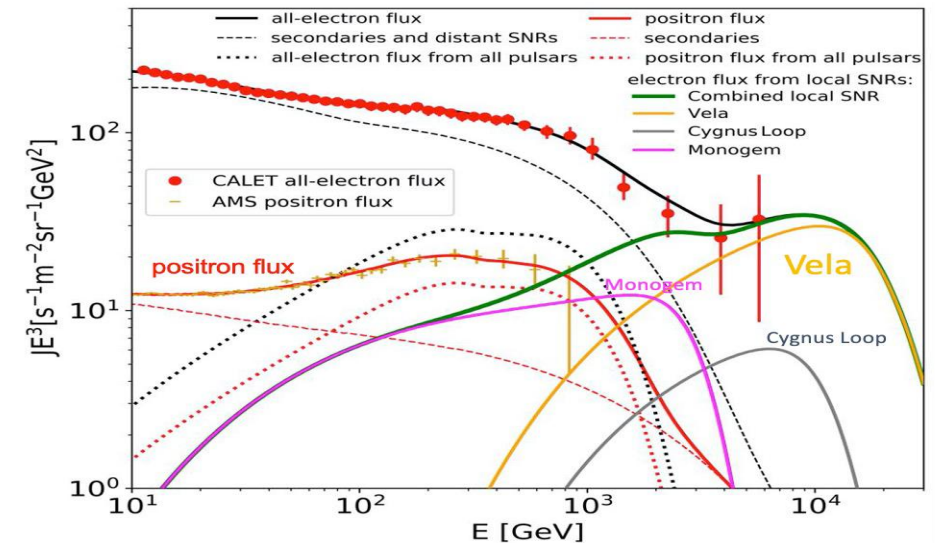
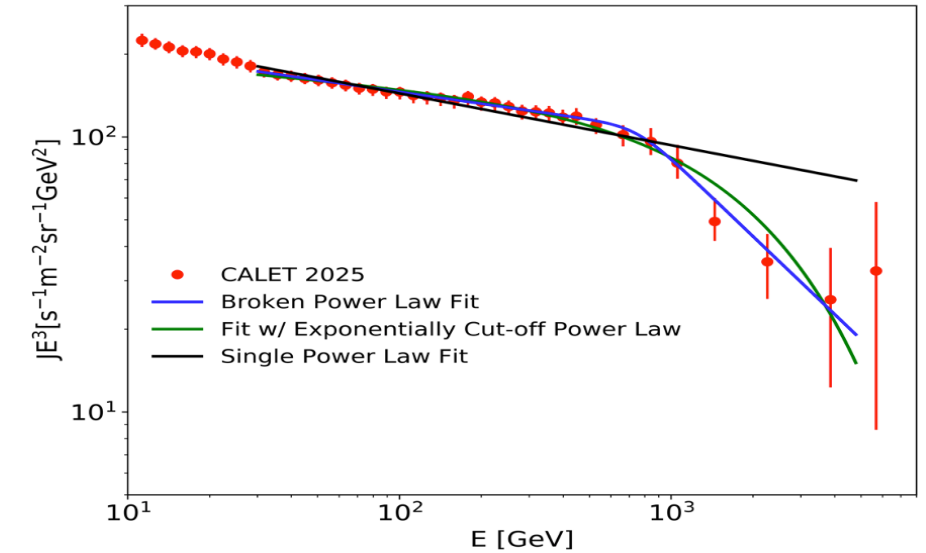
- More than 9 years observation has reduced statistics and systematic errors.
- Statistics has increases by 27% from PRL 2023.
- Systematic discrepancy between CALET/AMS-02 and DAMPE/Fermi-LAT remains.

CALET observes a flux suppression above 1 TeV with a **significance of 6.7σ** .



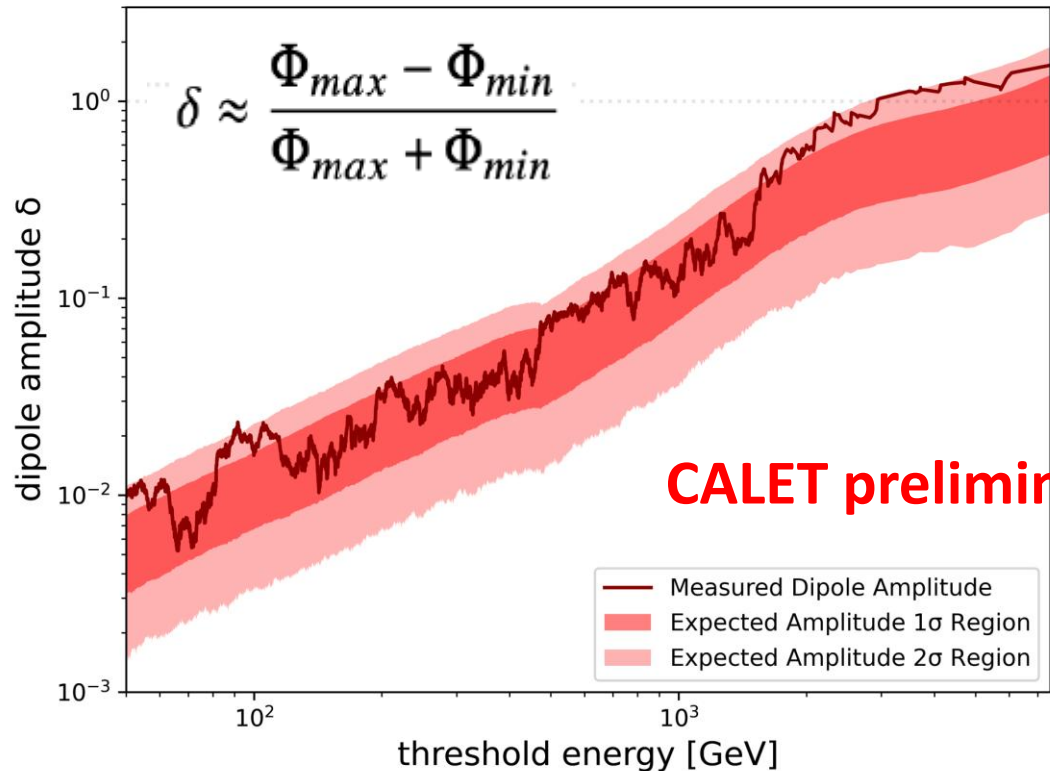
Towards an Interpretation of the CALET All-electron Spectrum

- Fit in 30-4.8TeV
 - Single power law is suppressed above 1 TeV with a significance $\sim 6.7\sigma$.
 - Broken power law
 - $\gamma = -3.14 \pm 0.01 \rightarrow 3.92$ at $752 \pm 140 \text{ GeV}$
($\chi^2/\text{NDF} = 1.7/28$)
 - Exponentially cut-off power law
 - $\gamma = -3.10 \pm 0.01$ at $2854 \pm 304 \text{ GeV}$
($\chi^2/\text{NDF} = 6.1/28$)
- Possible spectral fit in whole energy region
 - Positron contribution is fitted using AMS flux with secondaries + pulsers.
 - CALET electron+positron flux is fitted with secondaries + pulsers + SNRs.



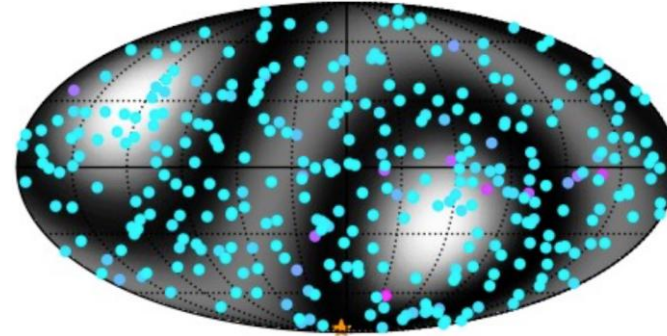
Dipole Anisotropy Measurement

Data sample: 3×10^5 electrons above 50 GeV
(Oct. 2015 – Dec. 2024)

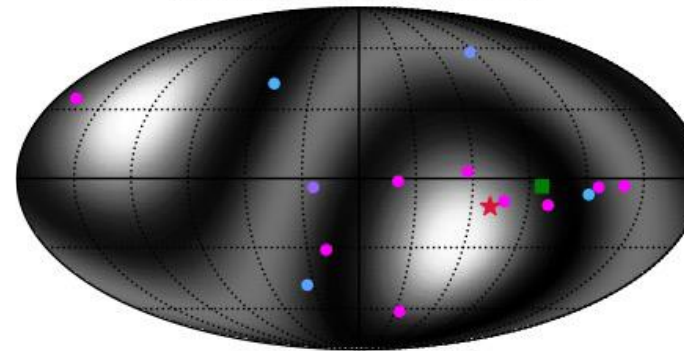


Dipole amplitude is within 2 σ band. But the amplitude above ~ 2 TeV is close to the upper boundary.

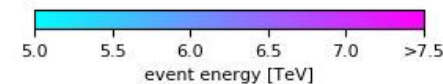
event map in $E > 1$ TeV



event map in $E > 5$ TeV

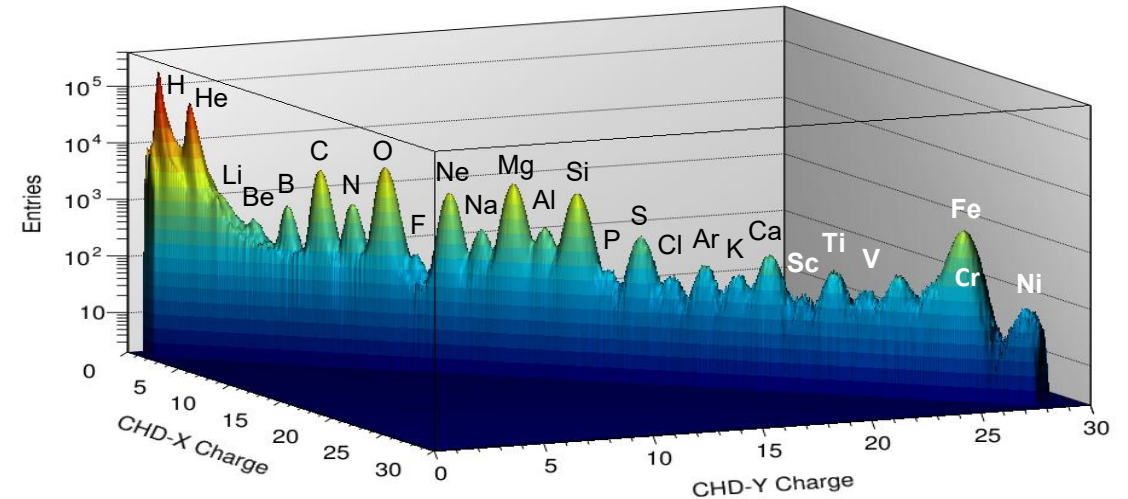
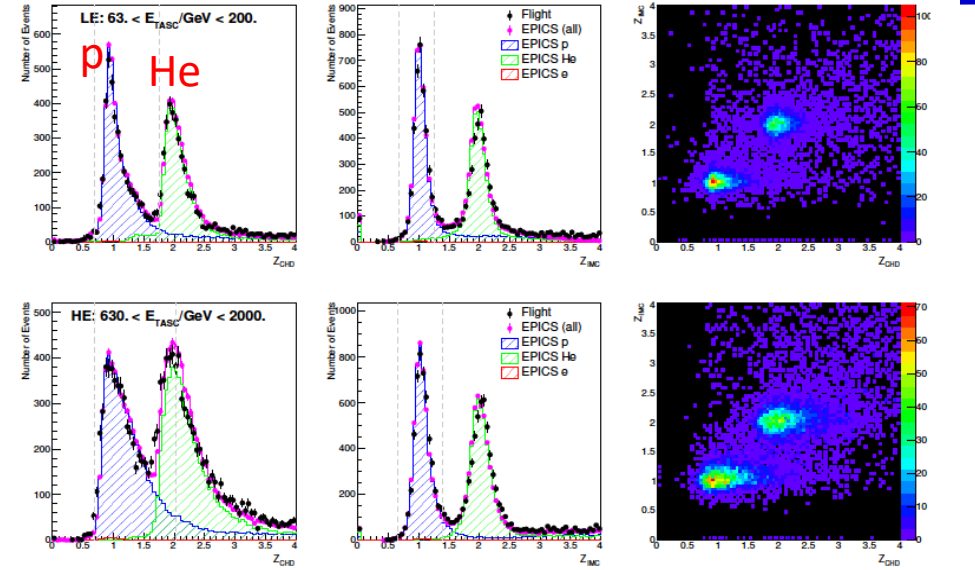
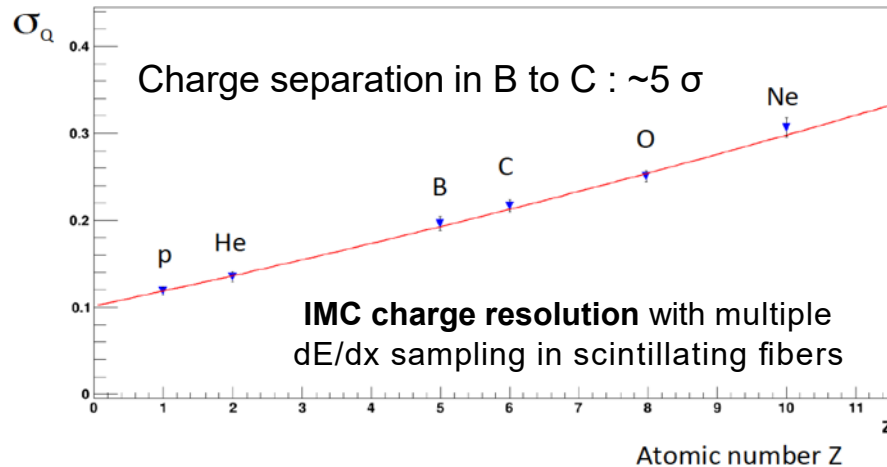
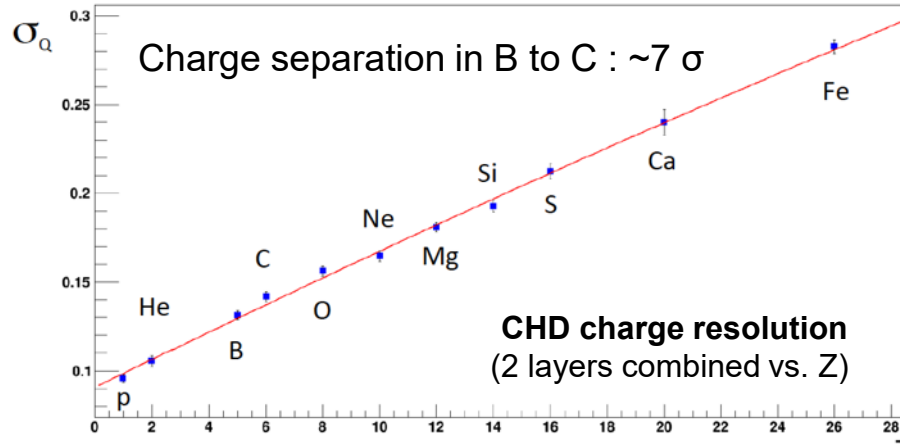


In $E > 5$ TeV, event cluster close to the direction toward the Vela SNR.

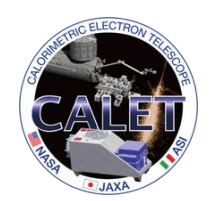


Charge Identification with CHD and MC

Single element identification for p, He and light nuclei is achieved by CHD+IMC charge analysis.

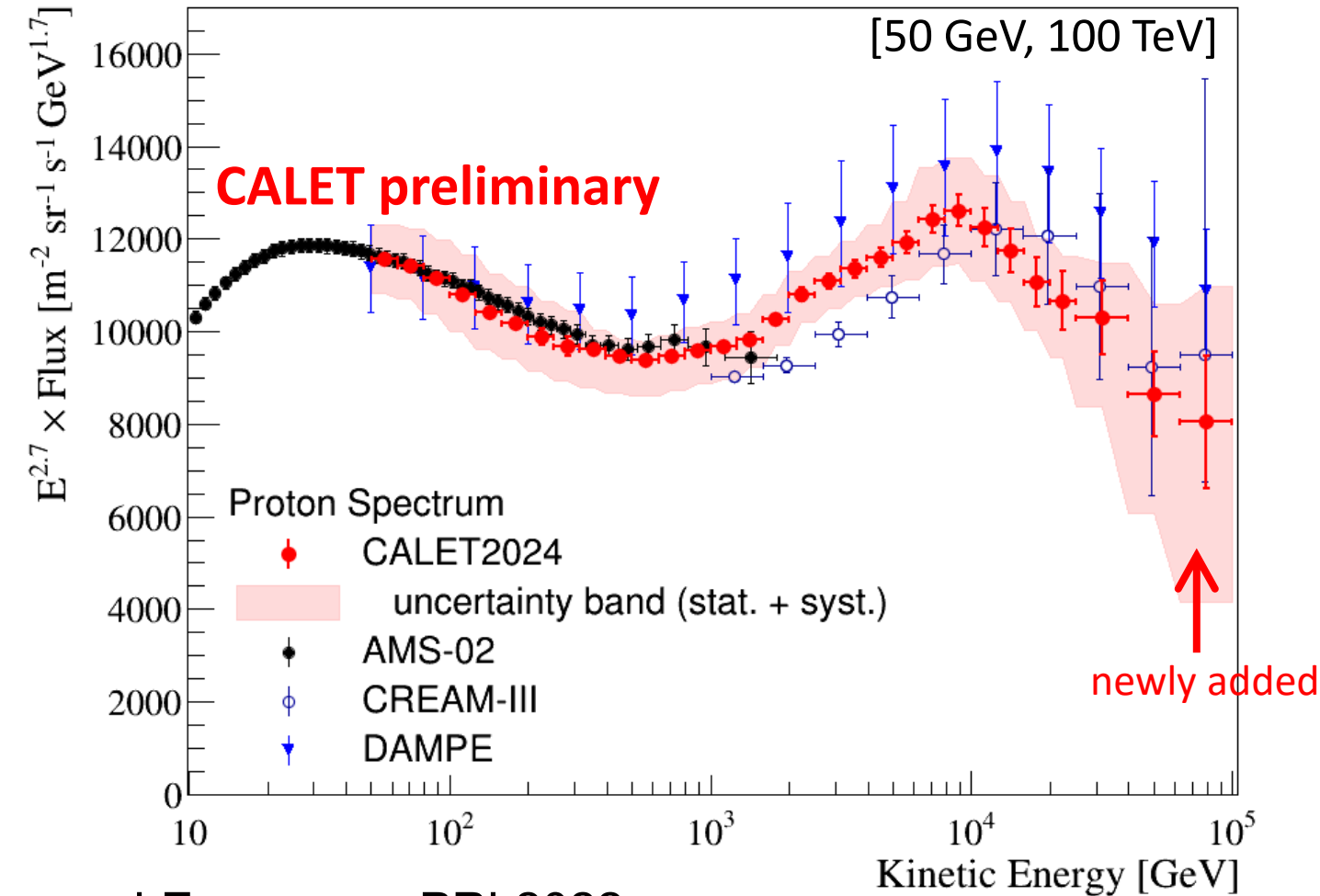


Deviation from Z^2 response is corrected both in CHD and IMC using a core + halo ionization model (Voltz)



Proton Energy Spectrum

PRL 129, 101102 (2022)
ICRC 2025 update



LE: same as PRL2022

HE: 2850 days of live time (Oct. 2015 – Dec. 2024)

$$\Phi(E) = \frac{N(E)}{S\Omega T\Delta E\varepsilon(E)}$$

$\Phi(E)$: proton flux

$N(E)$: number of events in ΔE bin (after background subtraction)

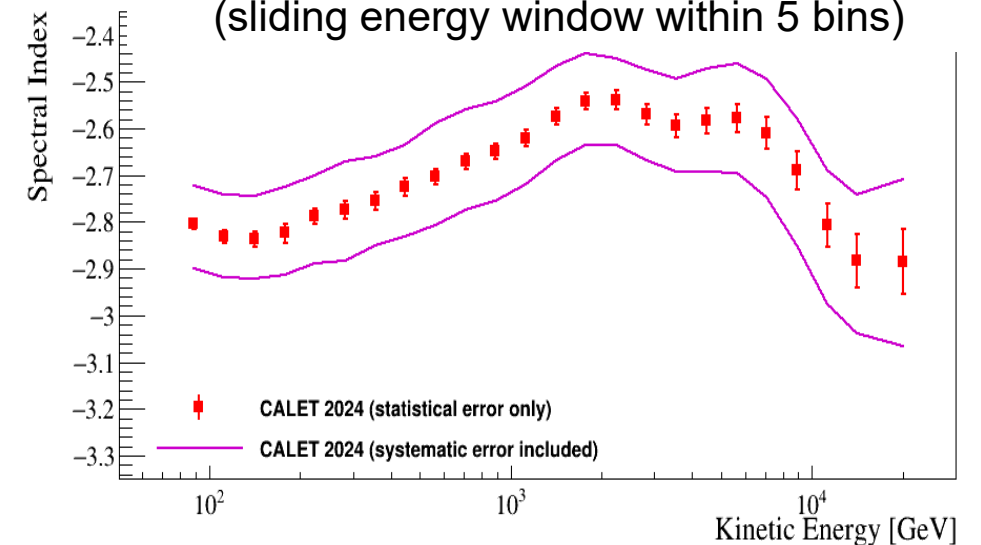
$S\Omega$: geometrical acceptance (510cm²sr)

T : livetime

ΔE : energy bin width

$\varepsilon(E)$: detection efficiency

Energy dependence of spectral index
(sliding energy window within 5 bins)

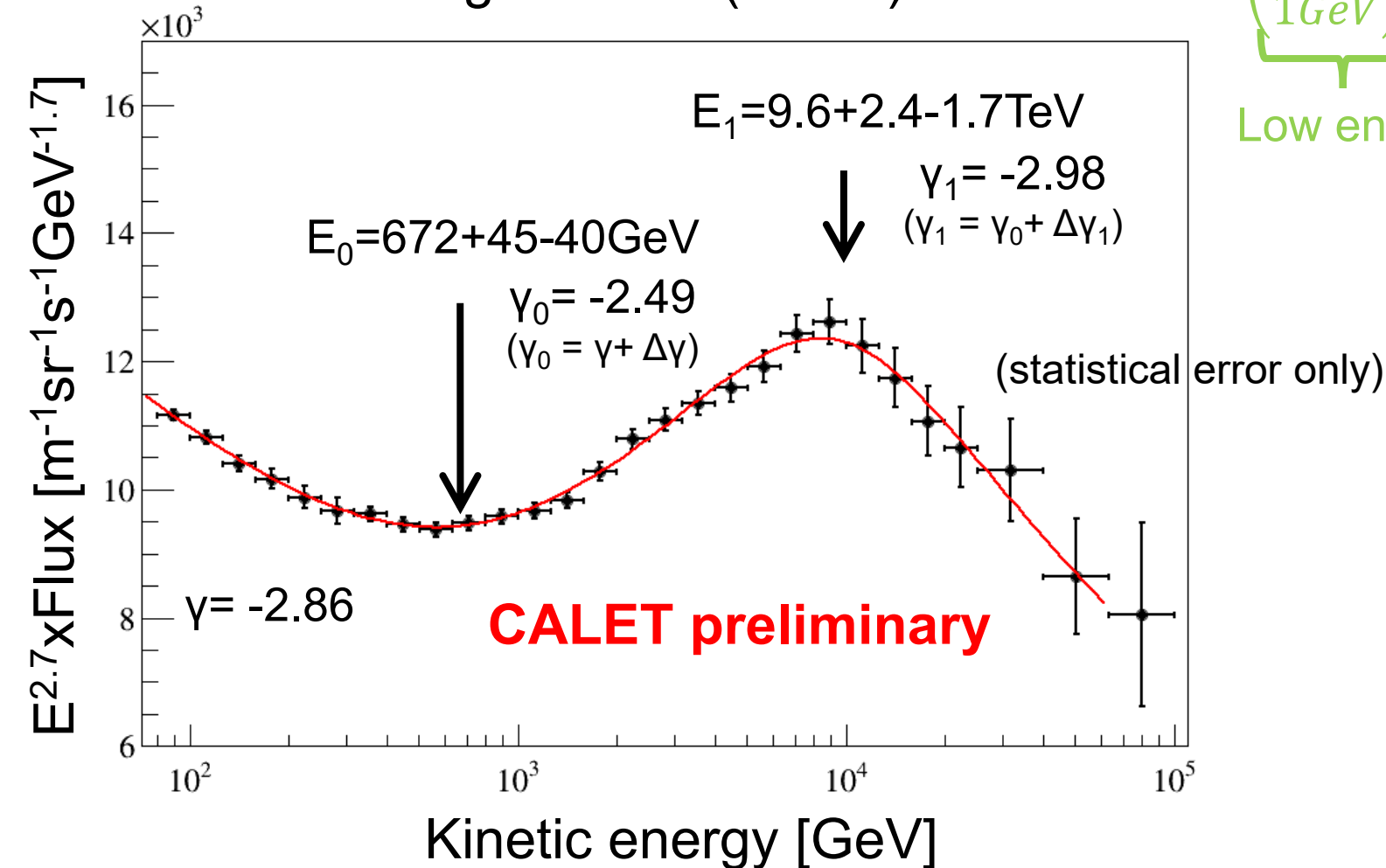




Spectral Fit with Double Broken Power Law (DBPL)

Fitting function (DBPL): $\Phi = E^{2.7} \times C \times \underbrace{\left(\frac{E}{1\text{GeV}}\right)^{\gamma}}_{\text{Low energy}} \times \underbrace{\left(1 + \left(\frac{E}{E_0}\right)^s\right)^{\frac{\Delta\gamma}{s}}}_{\text{hardening}} \times \underbrace{\left(1 + \left(\frac{E}{E_1}\right)^{s_1}\right)^{\frac{\Delta\gamma_1}{s_1}}}_{\text{softening}}$

$\chi^2 = 6.8/20$



| | |
|------------------|-------------------------------------|
| γ | $-2.858 + 0.005 - 0.005$ |
| s | 1.6 ± 0.2 |
| $\Delta\gamma$ | $(3.7 \pm 0.1) \times 10^{-1}$ |
| E_0 | $(6.72 + 0.45 - 0.40) \times 10^2$ |
| $\Delta\gamma_1$ | $(-4.9 + 1.2 - 1.3) \times 10^{-1}$ |
| E_1 | $(9.6 + 2.4 - 1.7) \times 10^3$ |
| s_1 | $2.7 + 3.5 - 0.5$ |

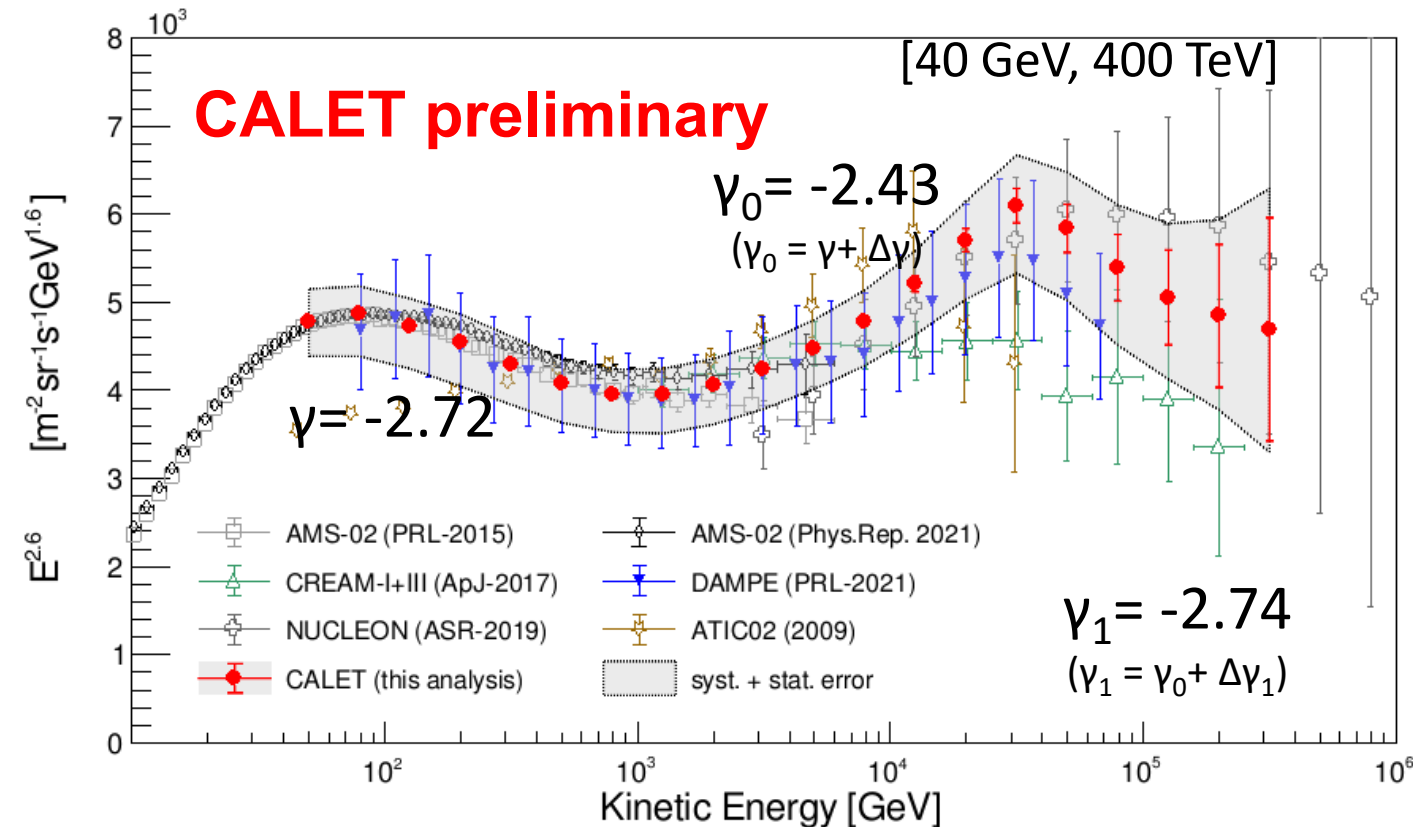
The s_1 becomes smoother,
but s_1 is larger than s .



Helium Energy Spectrum

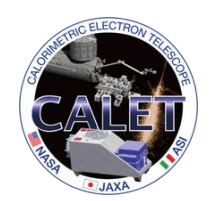
PRL 130, 171002 (2023)
ICRC2025 update

Data: Oct. 2015 – Sep. 2020



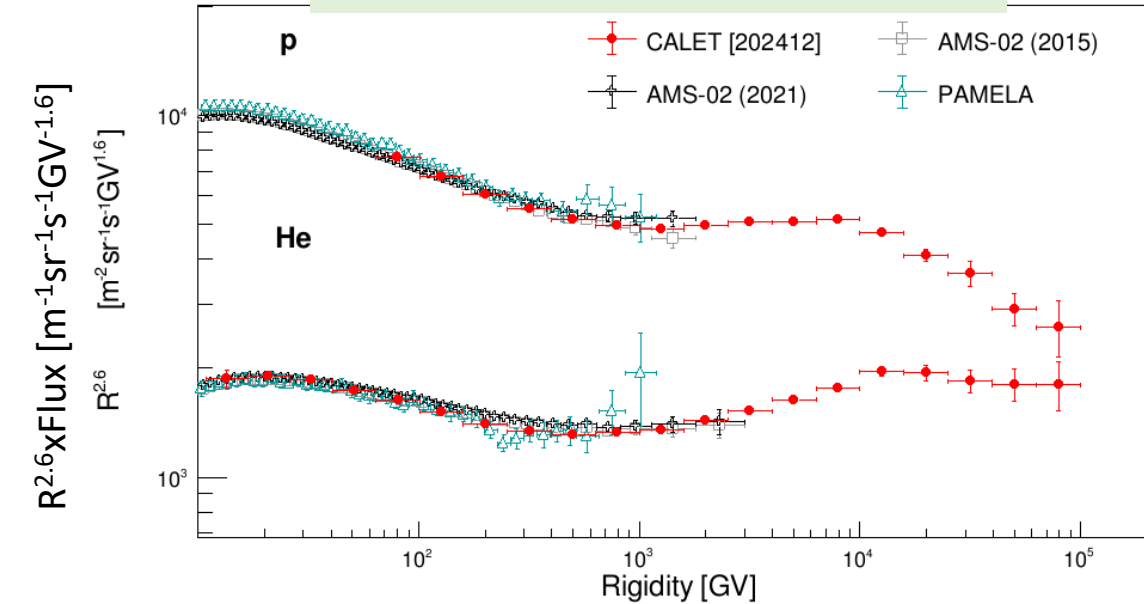
- We observe the spectral hardening starting at
 $E_0 = 1.276^{+0.111}_{-0.094}(stat)^{+0.250}_{-0.198}(sys) \text{ TeV}$
 This is consistent with DAMPE result (PRL 2021).
- We also observe spectral softening starting at
 $E_1 = 34.6^{+7.2}_{-5.5}(stat)^{+1.6}_{-6.1}(sys) \text{ TeV}$

$$\Phi'(E) = C \times \left(\frac{E}{1 \text{ GeV}} \right)^\gamma \times \left[1 + \left(\frac{E}{E_0} \right)^s \right]^{\frac{\Delta\gamma}{s}} \times \left[1 + \left(\frac{E}{E_1} \right)^{s_1} \right]^{\frac{\Delta\gamma_1}{s_1}}$$

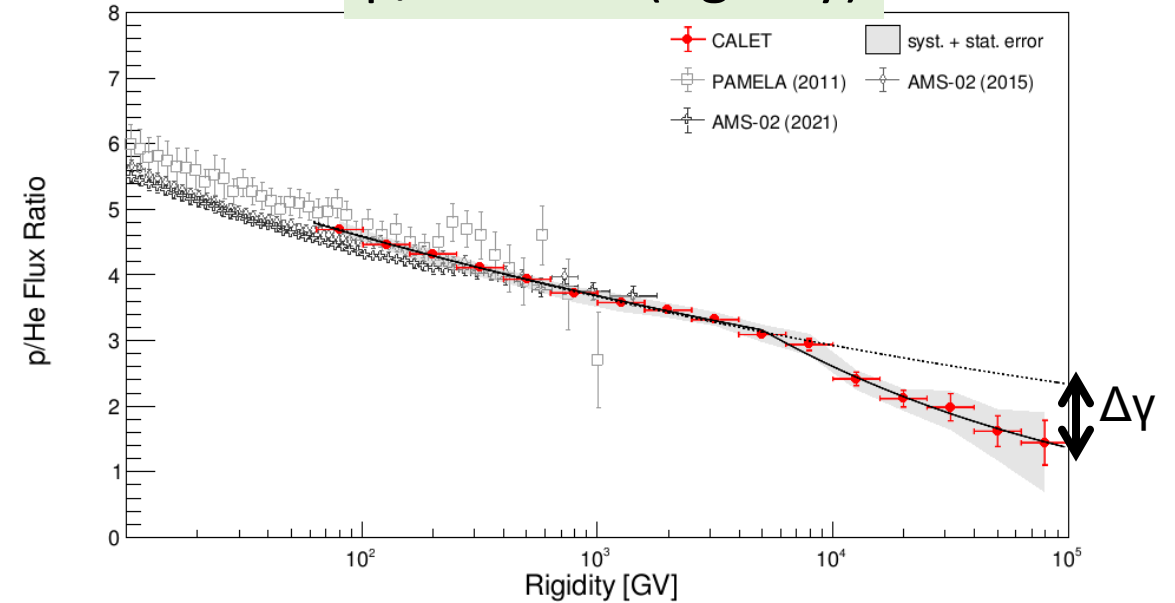


Proton/He ratio

p and He fluxes (rigidity)



p/He ratio (rigidity)



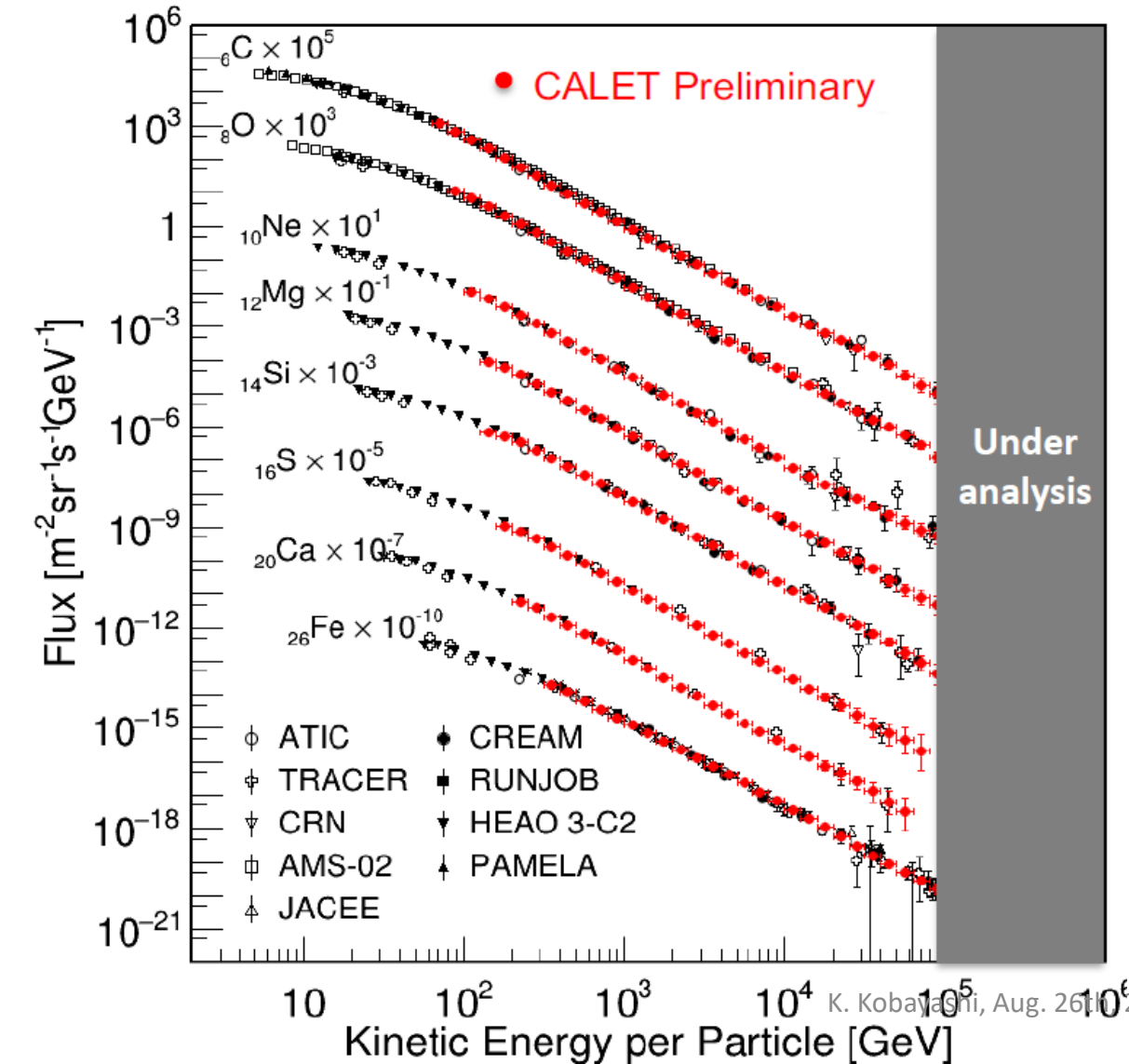
- Spectral hardening in rigidity are consistent between proton and helium.
- p/He ratio from tens GV to 10 TV is well described by SPL ($\Phi(R) = A \times R^\gamma$, $\gamma = -0.097 \pm 0.005$).
- DPL is favored with a significance of 4.8σ compared to SPL from 60 GV to 100 TV.

$$\text{DPL: } \Phi(R) = \begin{cases} C \times \left(\frac{R}{1\text{GV}}\right)^\gamma & (R < R_0) \\ C \times \left(\frac{R}{1\text{GV}}\right)^\gamma \times \left(\frac{R}{R_0}\right)^{\Delta\gamma} & (R > R_0) \end{cases}$$

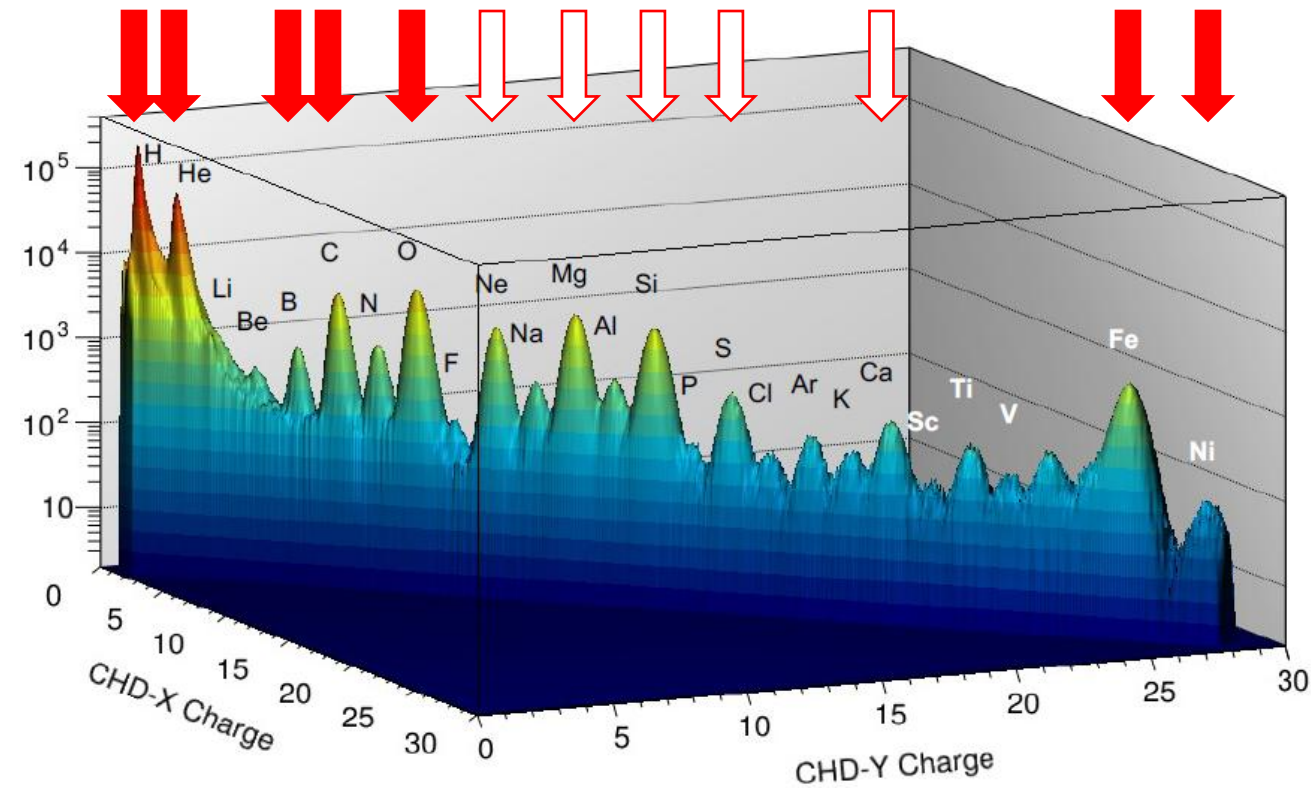
| | |
|----------------|----------------------------|
| γ | -0.097 ± 0.006 |
| R_0 | $6.60 \pm 1.87 \text{ TV}$ |
| $\Delta\gamma$ | -0.23 ± 0.08 |

Observations of Cosmic-ray Nuclei

Preliminary spectra of Carbon – Iron



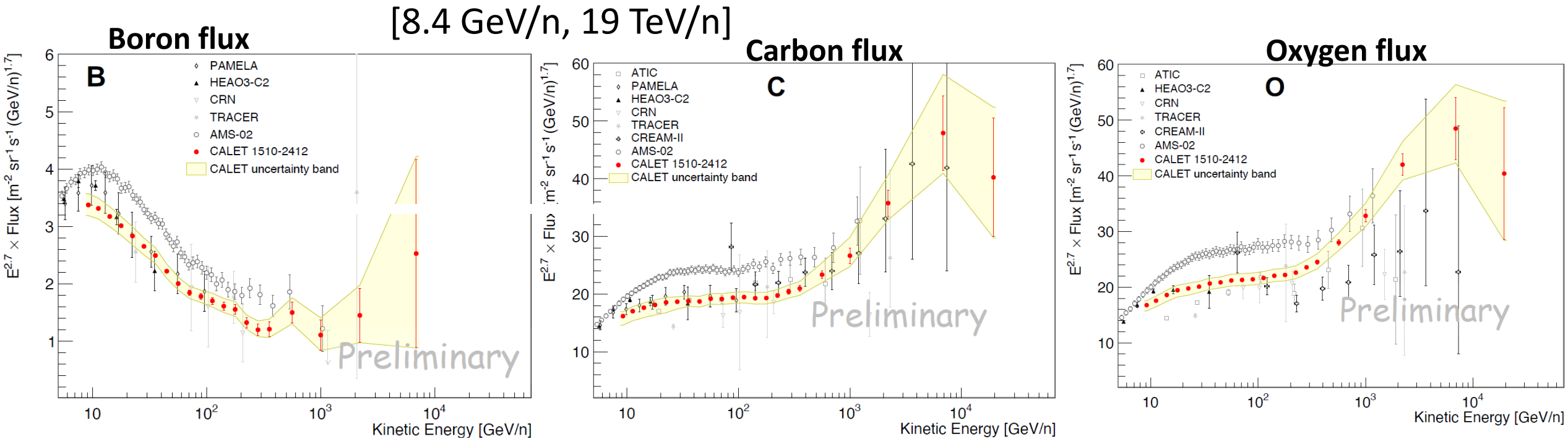
Dedicated analysis of cosmic-ray nuclear fluxes and flux ratios into the TeV region ongoing.





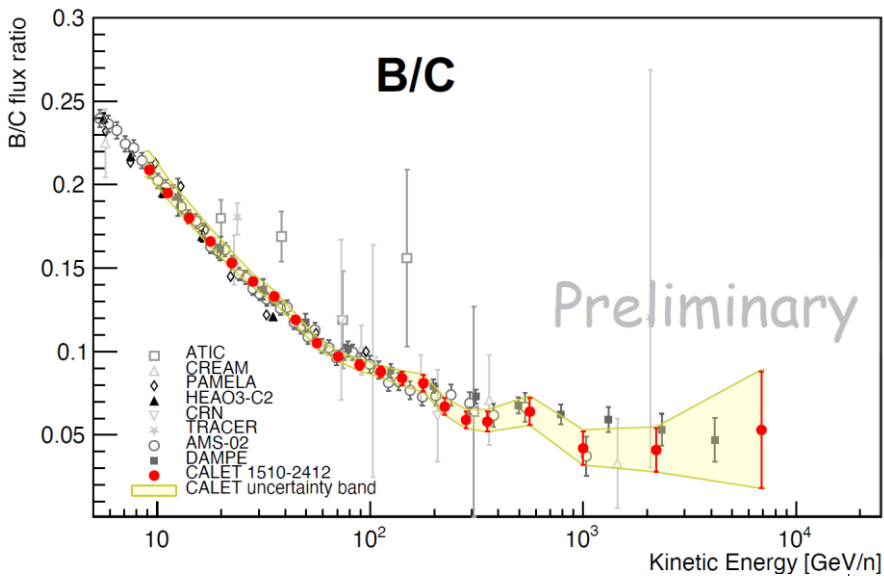
Energy Spectra of Cosmic-ray BCO

C&O: PRL 125, 251102 (2020)
B: PRL 129, 251103 (2022)
ICRC 2025 update

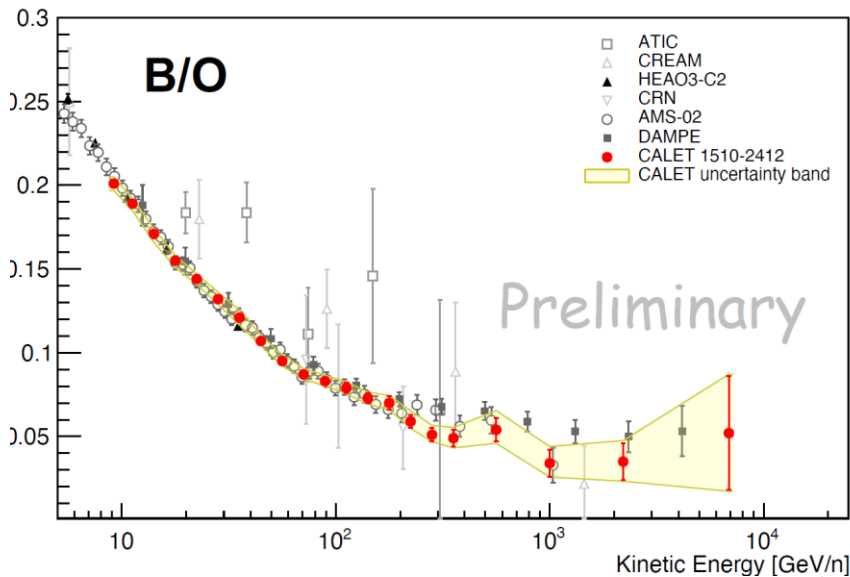


- CALET B,C are consistent with PAMELA and most of the previous experiments (PAMELA did not publish oxygen).
- CALET B,C,O absolute normalization are lower than AMS-02.
- The C, O spectra show a clear hardening around 200 GeV/n and hint of a softening around 10 TeV/n.

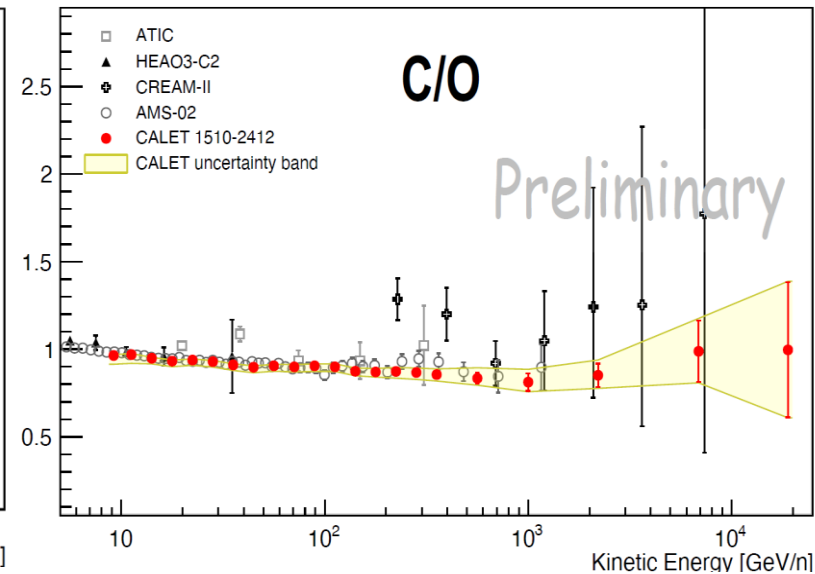
Boron / Carbon



Boron / Oxygen



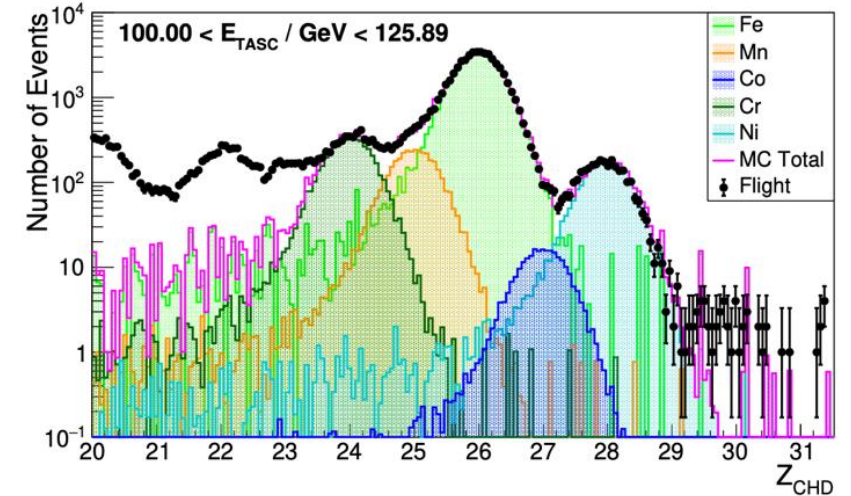
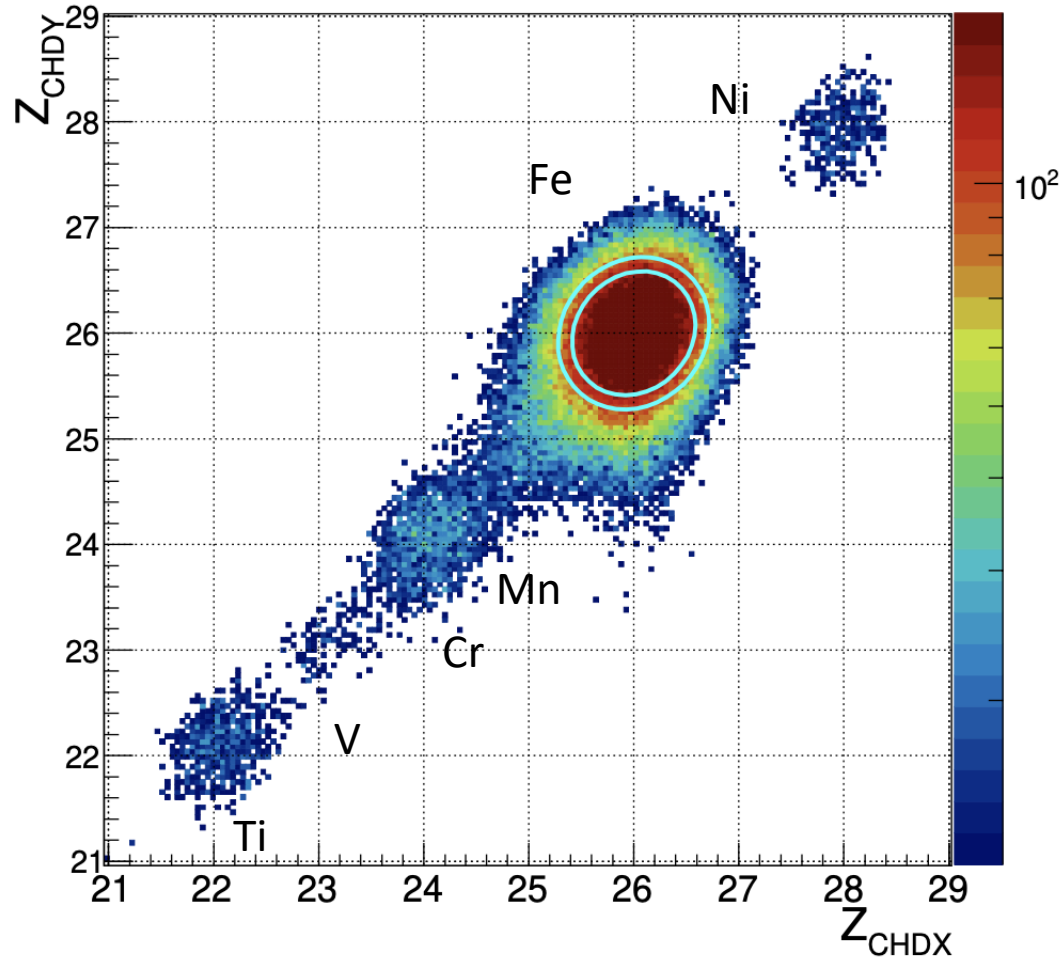
Carbon / Oxygen



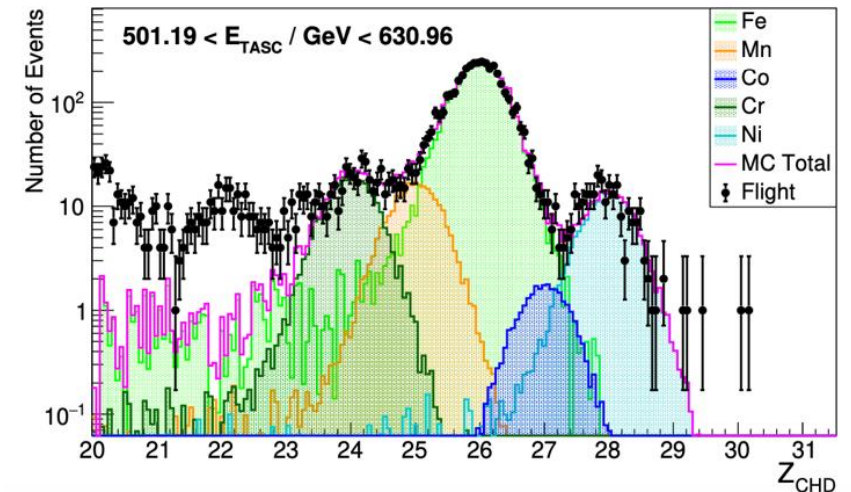
- Cosmic ray Boron are entirely produced by the collision with the interstellar matter, though carbon are thought to be mainly produced and accelerated in astrophysical sources. Therefore, B/C ratio directly measures the average amount of interstellar material traversed by cosmic rays.
- B/C, B/O, and C/O ratio are consistent to AMS-02.

Iron – Analysis (Charge Selection)

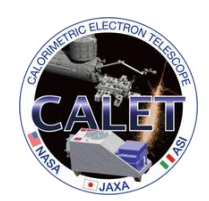
Charge measurement with the two CHD layers



(a)



(b)



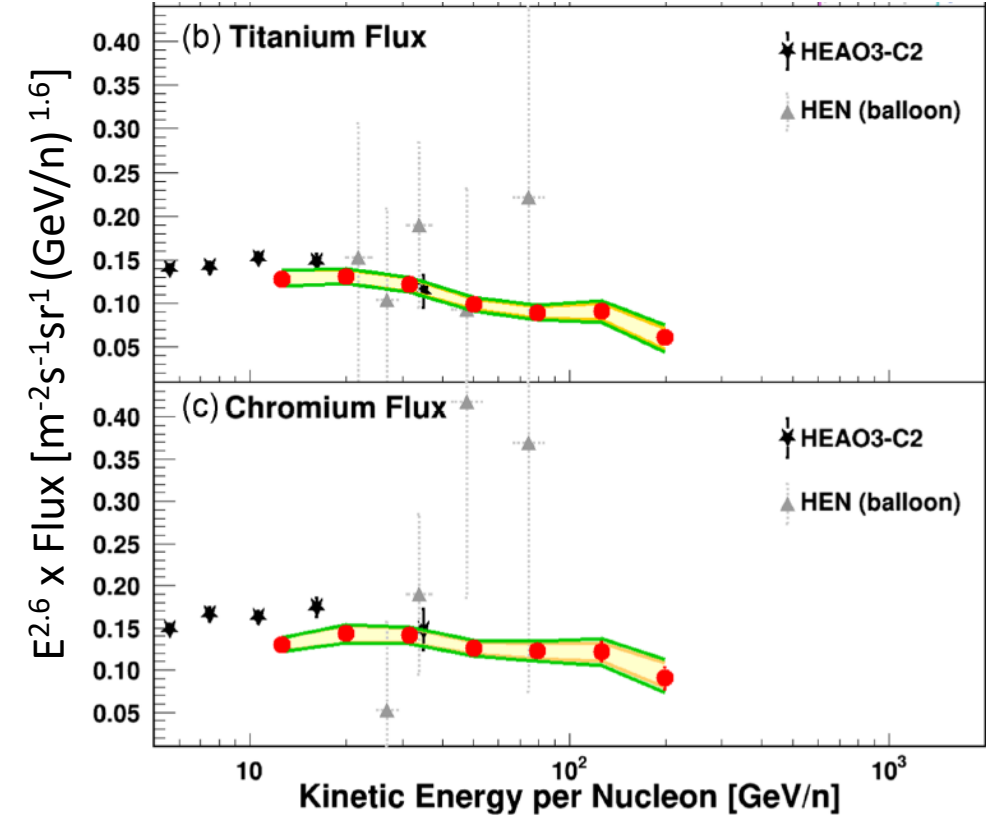
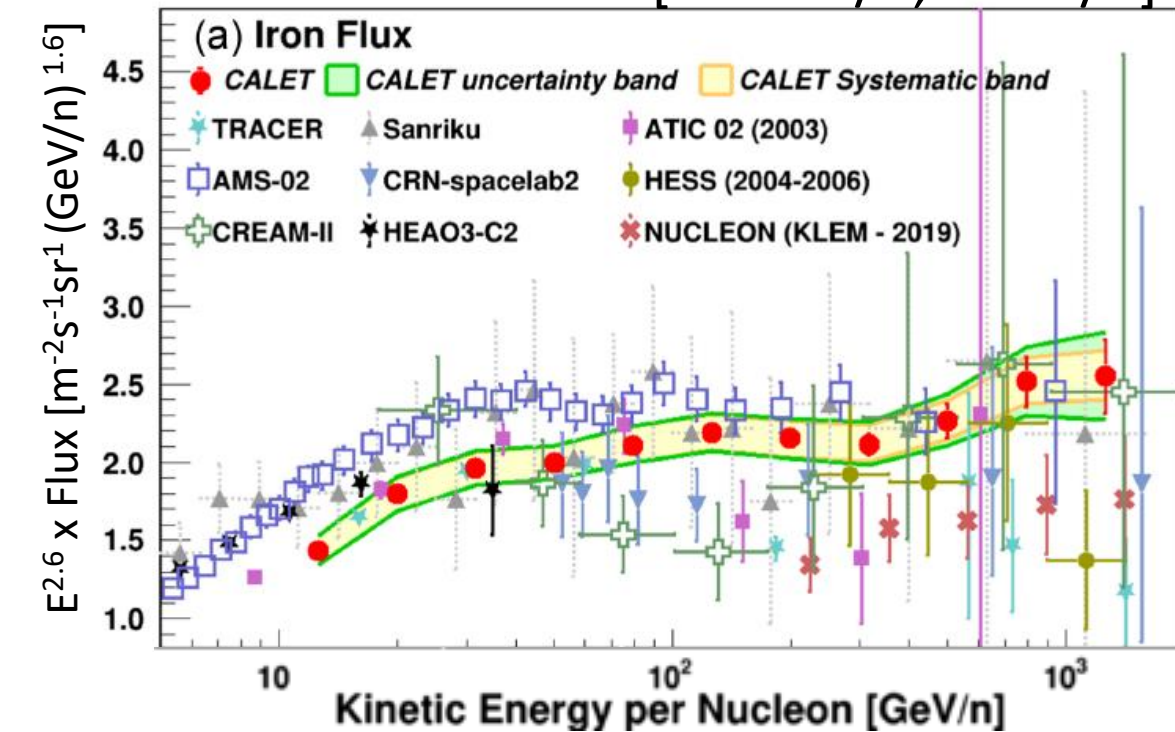
Iron and Sub-Iron Energy Spectrum

PRL 135, 021002 (2025)

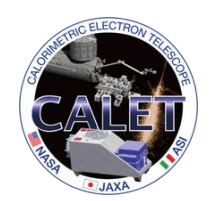
Data: Nov. 2015 – Oct 2023

[10 GeV/n, 100 GeV/n]

[10 GeV/n, 1 TeV/n]

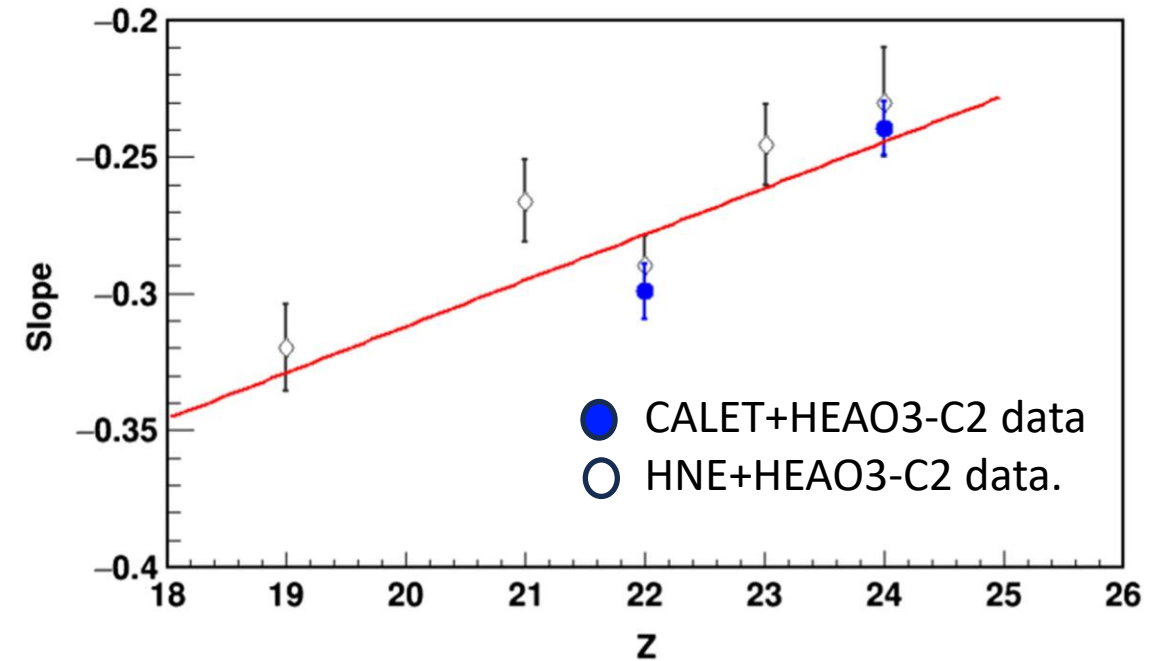
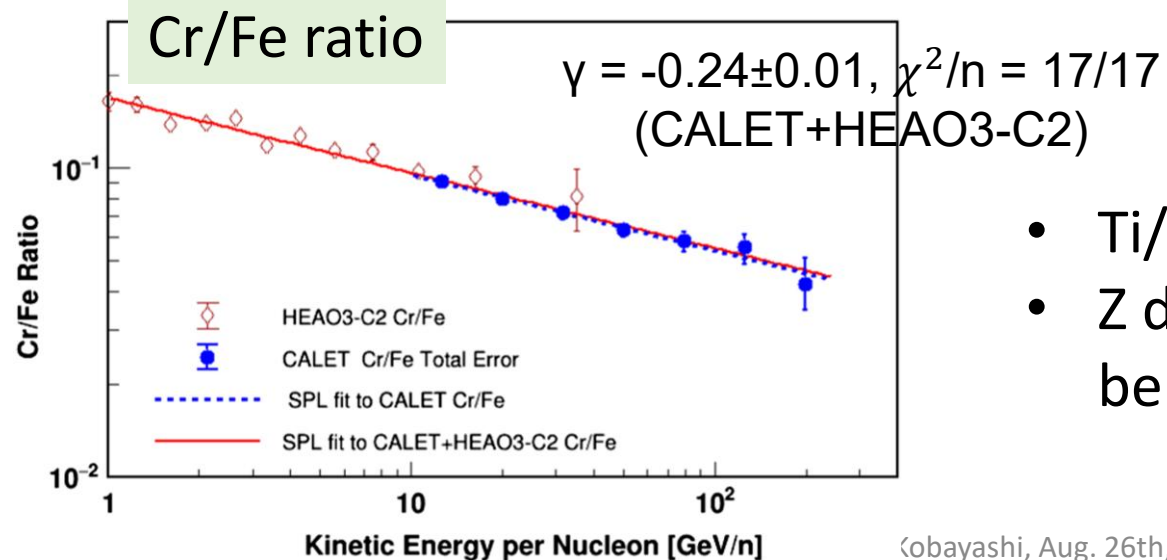
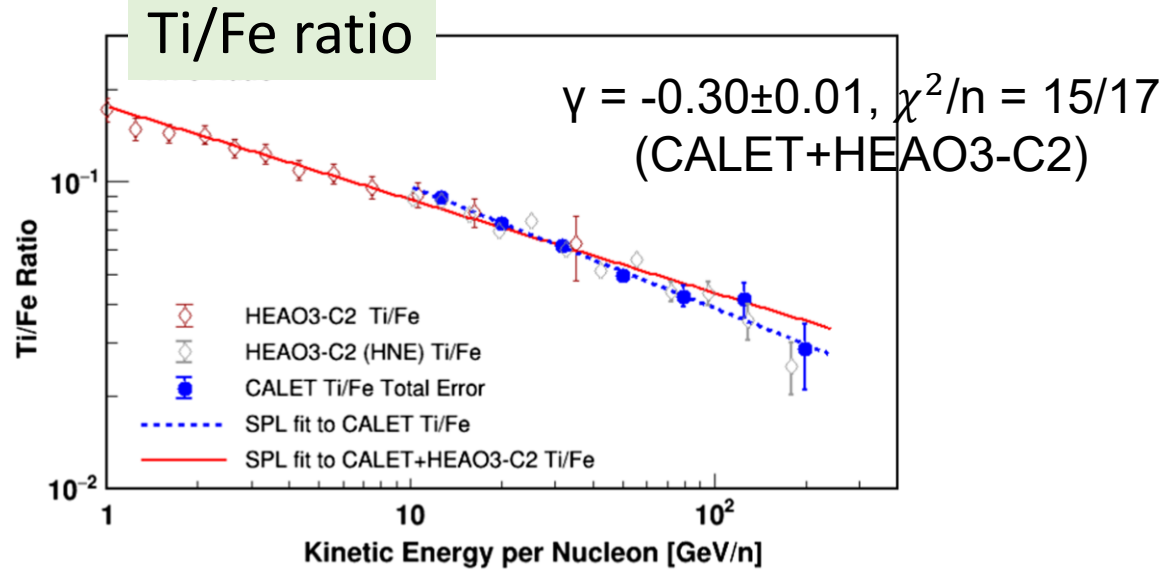


- Iron spectrum was updated with 2 times larger statistics than PRL 2020.
- Possible hardening of iron spectrum above a few hundred GeV/n.
- New measurement on Ti and Cr spectrum.

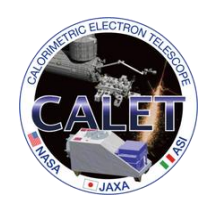


Sub-Iron to Iron Ratios

PRL 135, 021002 (2025)



- Ti/Fe and Cr/Fe ratios are well fitted with SPL.
- Z dependence of the Index of flux ratio is found to be consistent with the CALET + HEAO3-C2 data.

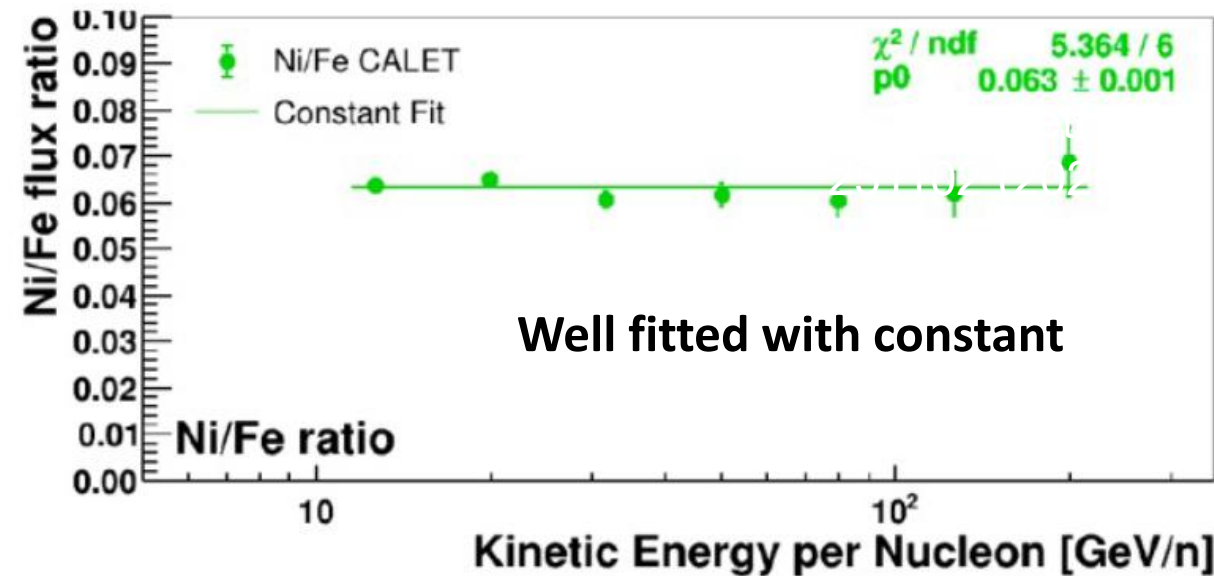
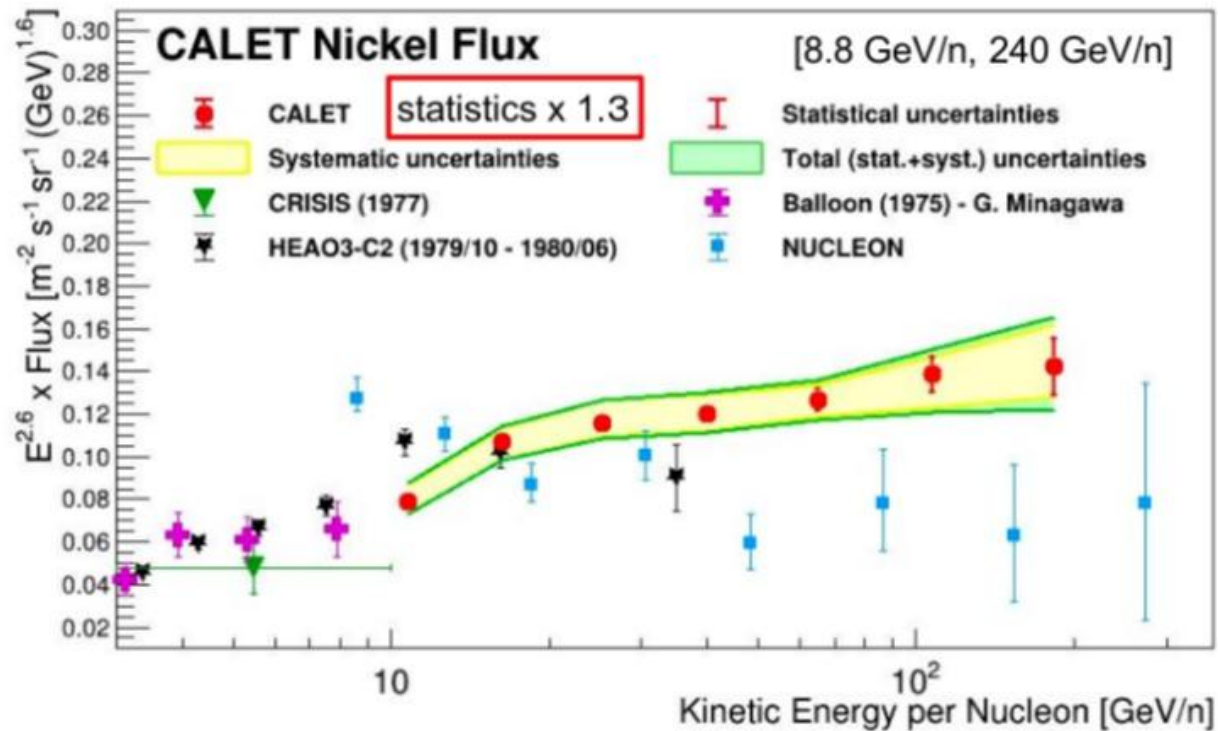


Nickel Energy Spectrum

PRL 128, 131103 (2022)
ICRC 2023 Update

Flux $\times E^{2.6}$ vs kinetic energy per nucleon [8.8 GeV/n, 240 GeV/n]

Data: Nov. 2016 – Dec 2022

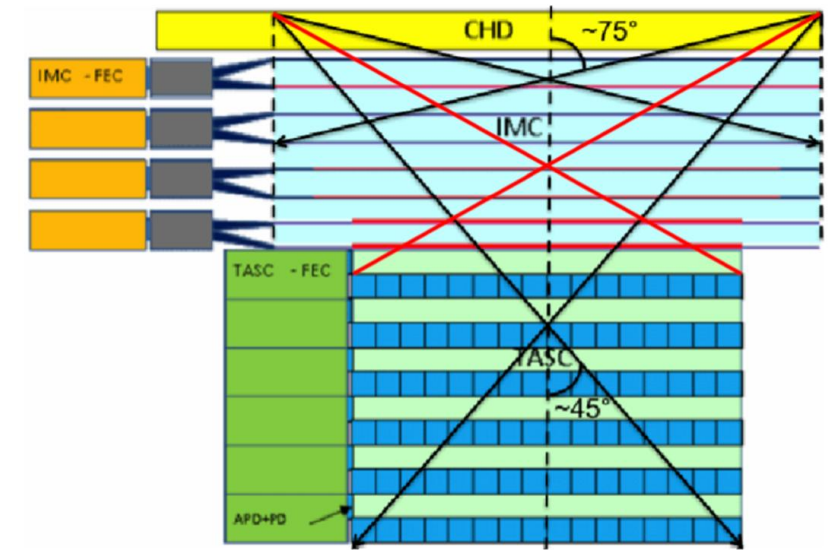
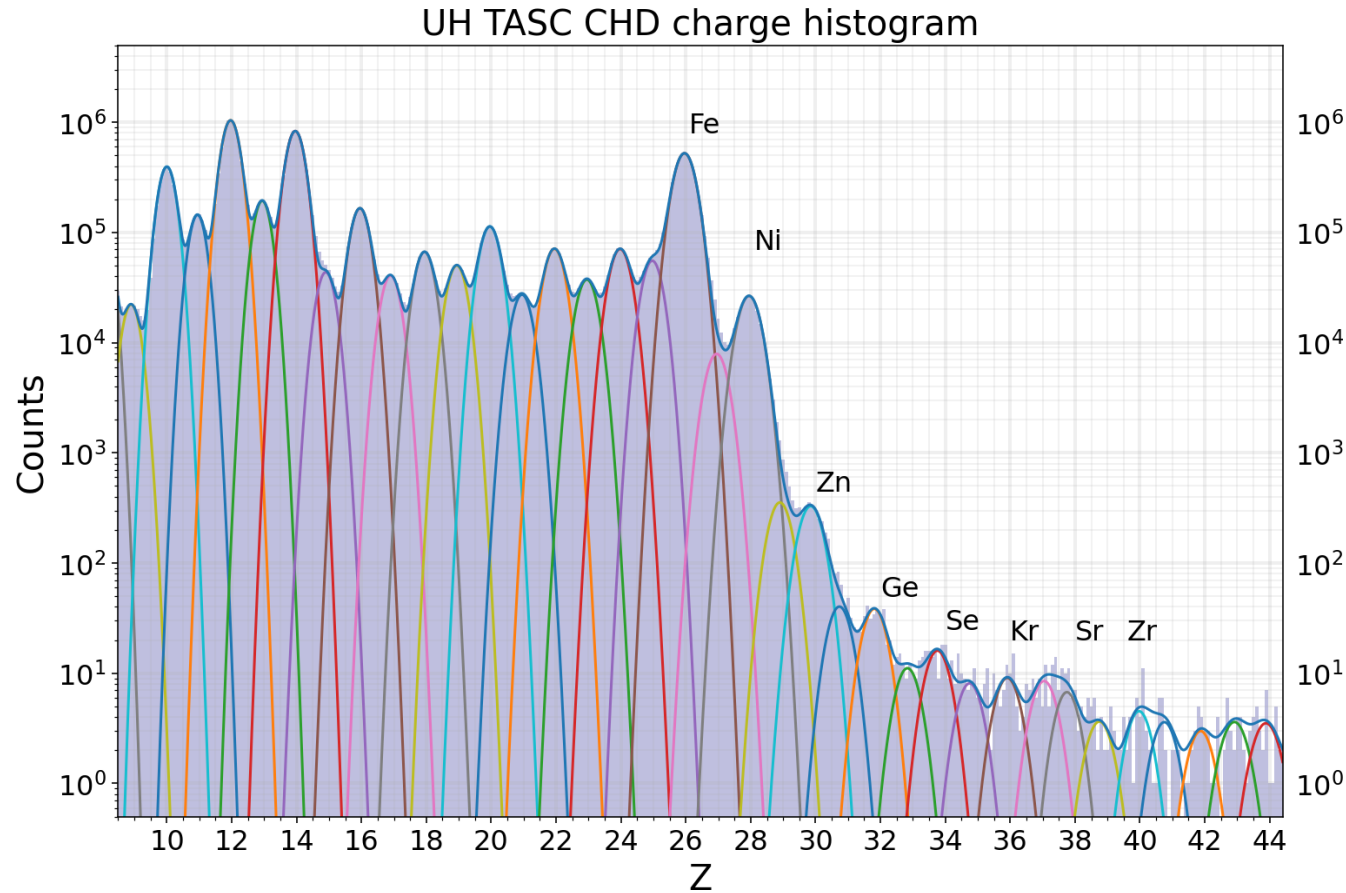


Ni and Fe fluxes have the same energy dependence.

Ultra Heavy Nuclei ($14 \leq Z \leq 44$)

APJ 988:148 (2025)

- Data: 7.5 years of CALET UH-trigger from Oct. 2015 to Nov. 2023.

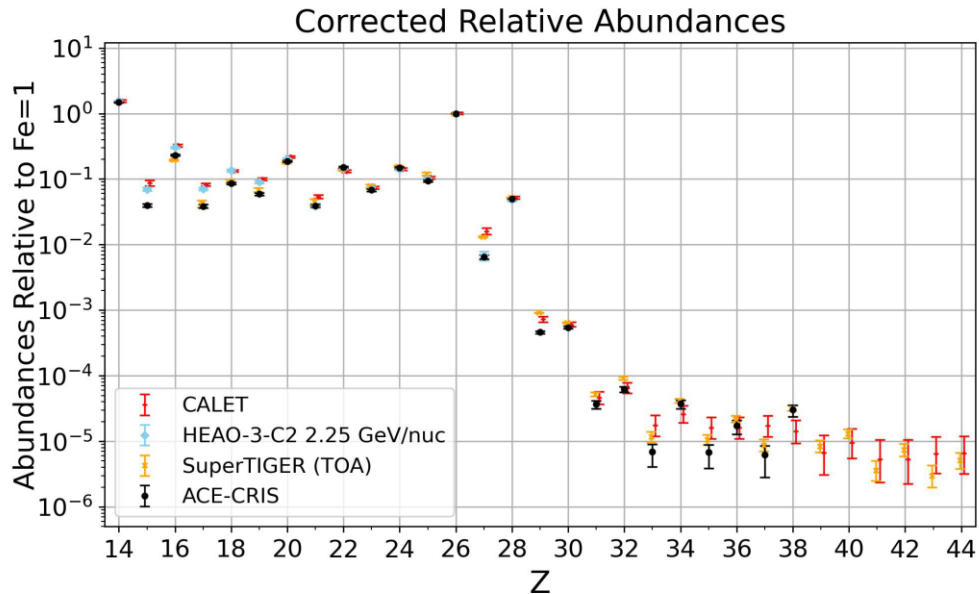


A special UH CR trigger uses the CHD and the first 4 layers of the IMC to achieve an expanded $\times 4$ geometric factor, $GF \sim 4400 \text{ cm}^2 \text{ sr}$.

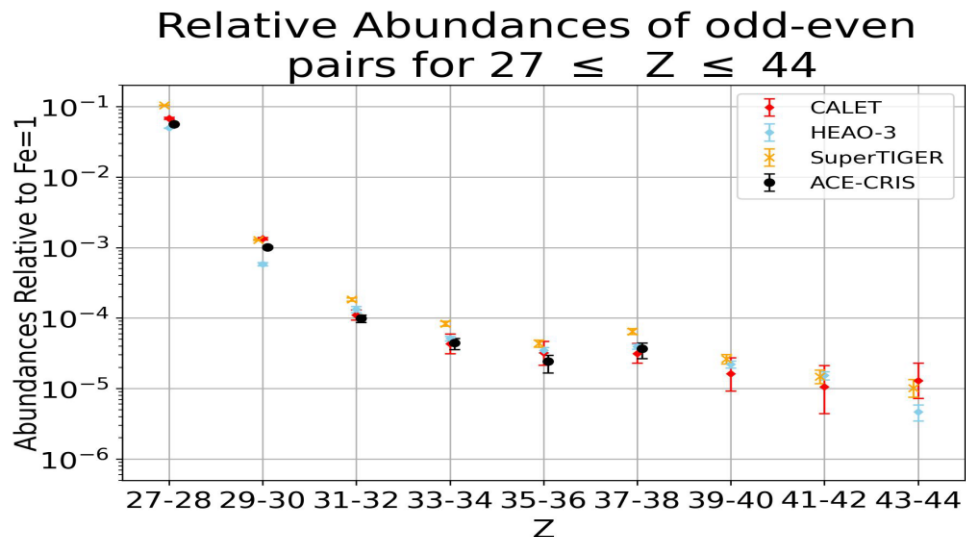


Ultra Heavy Nuclei ($14 \leq Z \leq 44$)

APJ 988:148 (2025)

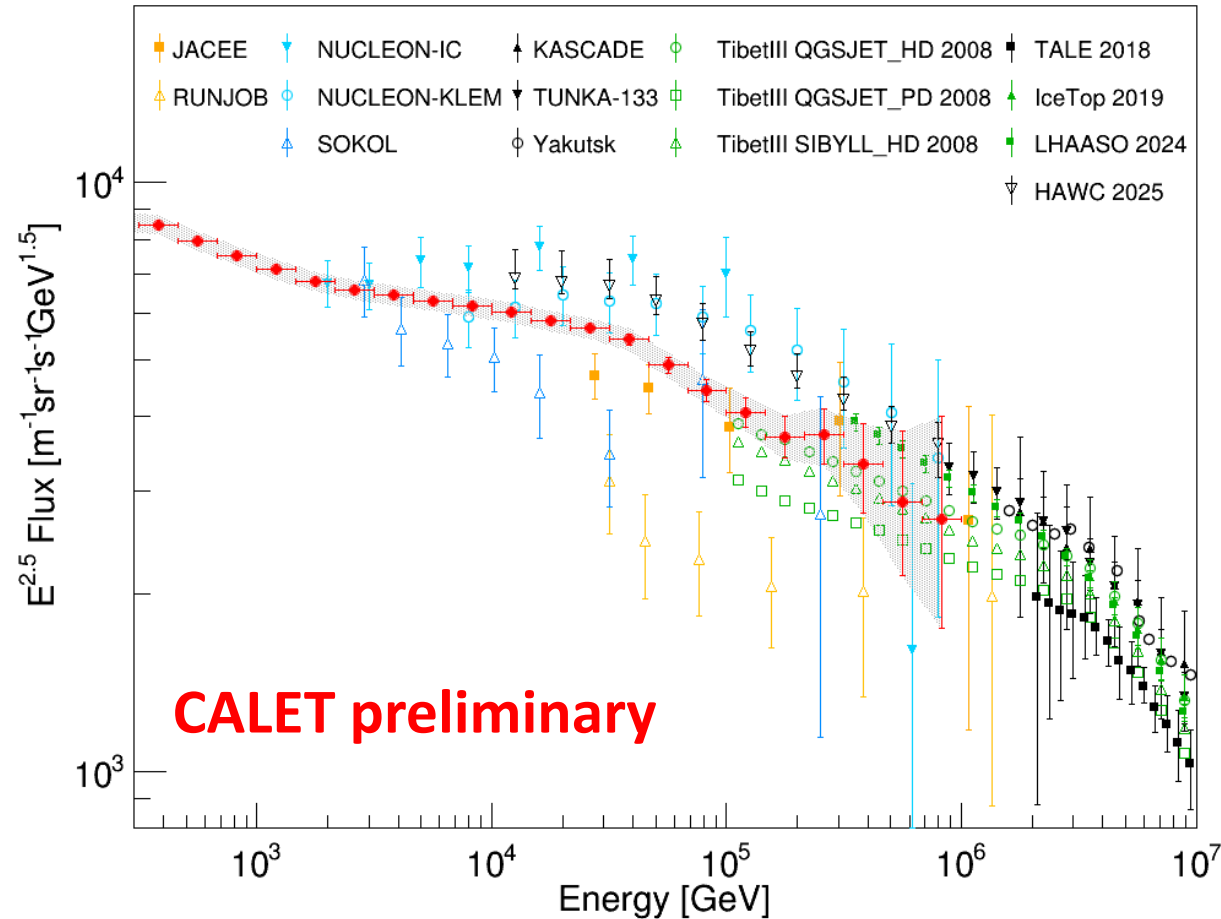


- We measure the relative abundances to Fe for $14 \leq Z \leq 44$.
- The CALET UH element ratios are consistent with Super-TIGER, ACE_CRIS, and HEAO-3 abundances.
- For $Z > 26$, odd peaks are higher than that of other experiments. However, relative abundance of odd-even elements pairs (lower figure) shows excellent agreement.

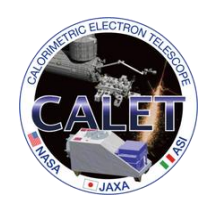


All-particle Spectrum from 31.6 GeV to 1 PeV ICRC2025

Data: Oct. 2015 – Dec. 2024



- Simple selection criteria are applied.
- MC (EPICS with DPMJET-III) are weighted to reproduce the fitted results of the observed CALET spectra.
- The spectrum is reconstructed using the unfolding response matrix from MC based on a weighted mixture of nuclei ($Z=1\sim 28$).
- CALET spectrum is close to the indirect measurements from ground experiments.



CALET GeV-energy Gamma Rays

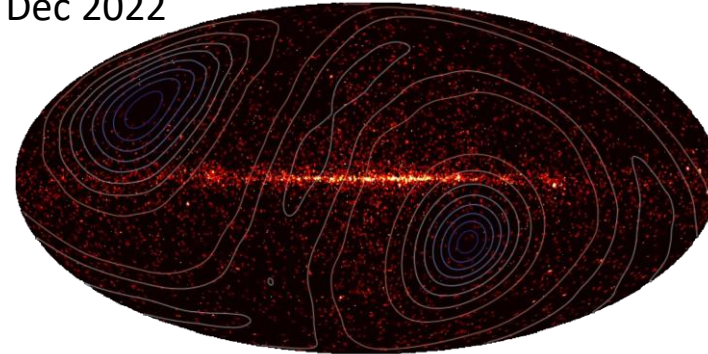
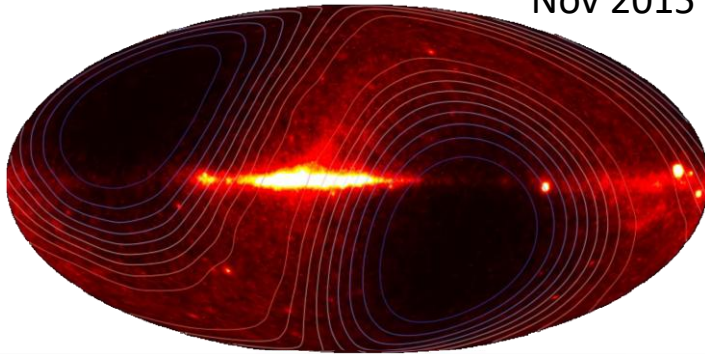
Effective area: $\sim 400 \text{ cm}^2$ ($> 2 \text{ GeV}$)

LE- γ trigger ($E > 1 \text{ GeV}$)

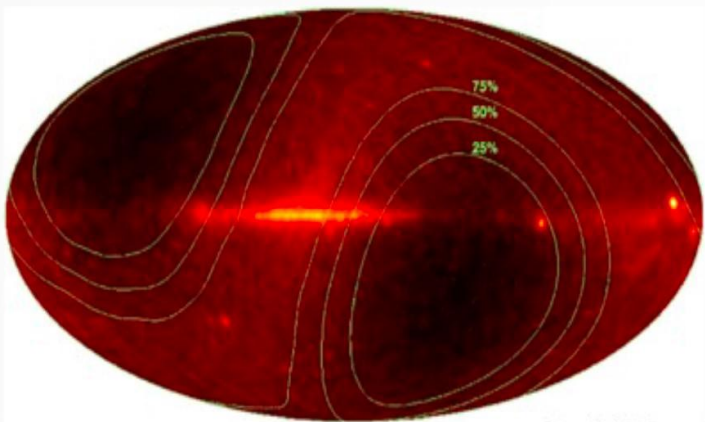
Angular resolution: $< 0.2^\circ$ ($> 10 \text{ GeV}$)

HE trigger ($E > 10 \text{ GeV}$)

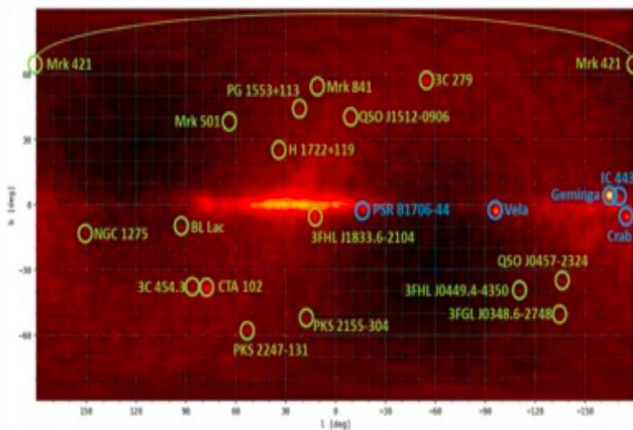
Nov 2015 – Dec 2022



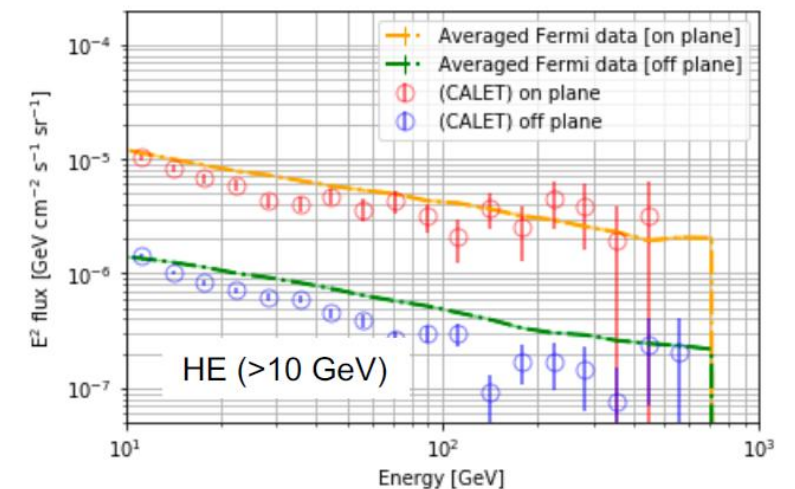
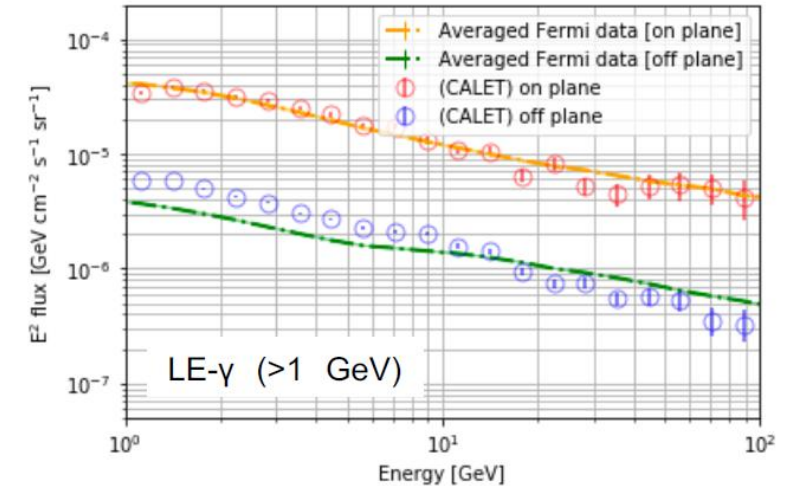
Gamma-ray sky map LE- γ trigger ($E > 1 \text{ GeV}$)



Identified bright point-sources ($E > 1 \text{ GeV}$)



Energy resolution: $\sim 2\%$ ($> 10 \text{ GeV}$)
Average galactic spectra



Measurements of energy spectra for point sources and diffuse structures are found to be consistent with those by Fermi-LAT.

K. Kobayashi, Aug. 26th, 2025, TAUP Xichang, Chengdu, China

On-plane: $|\ell| < 80^\circ$ & $|b| < 8^\circ$

Off-plane: $|b| > 10^\circ$

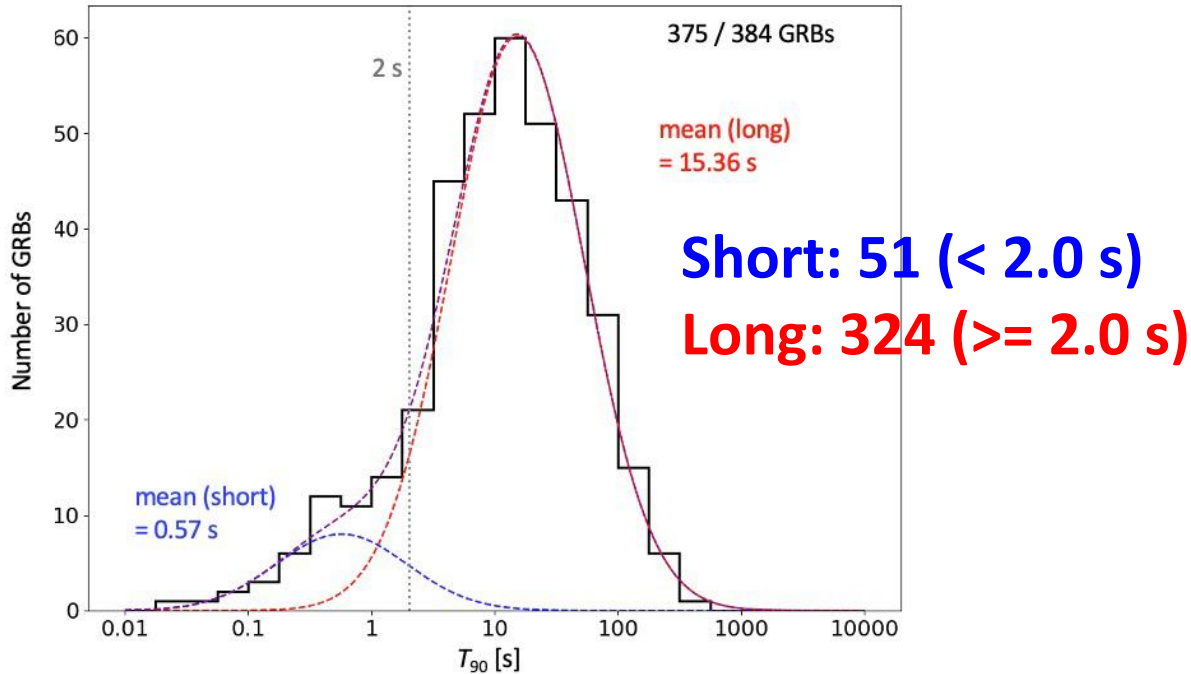


CALET Gamma-ray Burst Monitor

ICRC2025

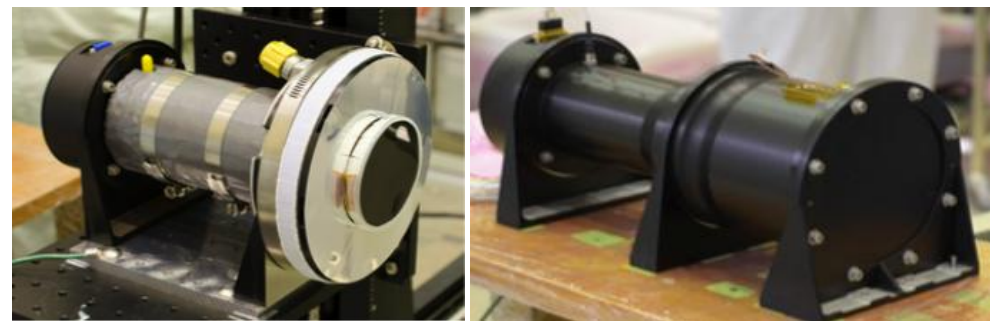
GRB search

CGBM has performed GRB observations on ISS for more than 9 years.
In Oct. 5th, 2015 – Apr. 30th, 2025, we have detected 365 GRBs.



CGBM detector

Hard X-ray Monitor Soft Gamma-ray Monitor
7 – 1000 keV 40 keV – 20 MeV



Searched for electromagnetic counterparts of GW events in O4.

| | Detection (SNR>=7) | No detection | HV off | Outside of FOB |
|-----------------|--------------------|--------------|-----------|----------------|
| O4a | 0 | 44 | 37 | 4 |
| O4b | 1* | 51 | 47 | 7 |
| O4c | 0 | 8 | 7 | 2 |
| O4 total | 1 | 103 | 91 | 13 |

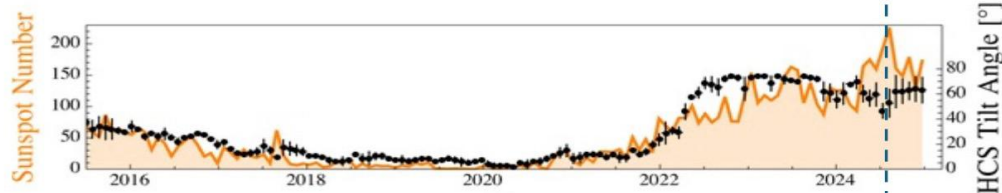
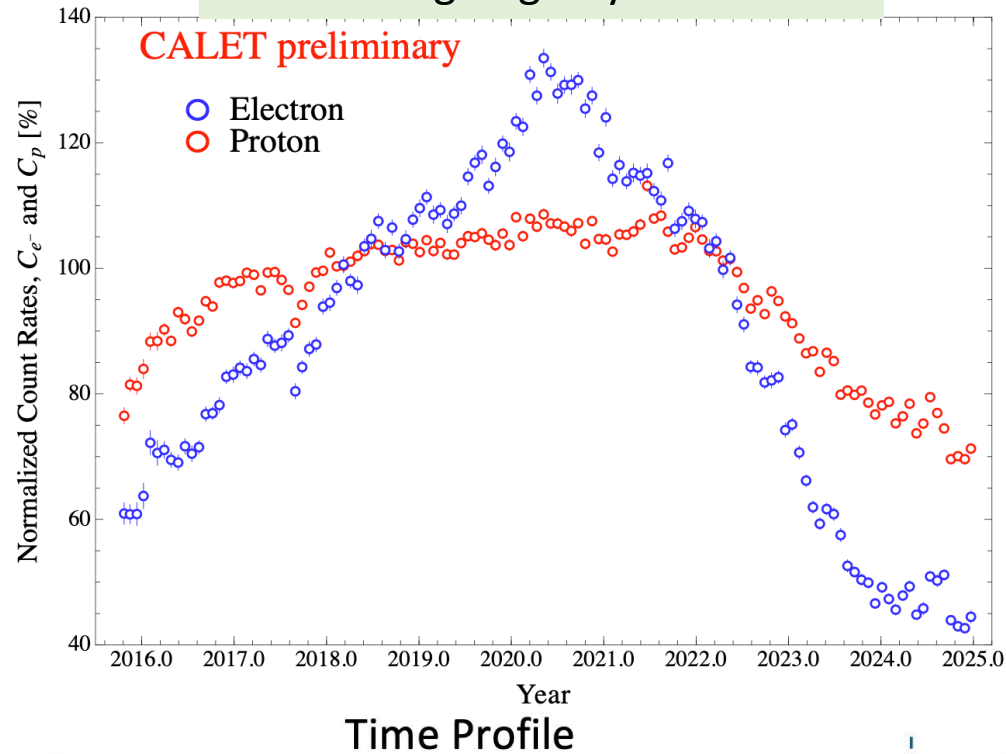
As of the end of April 2025, no GW candidates.



Charge-sign Dependent Solar Modulation

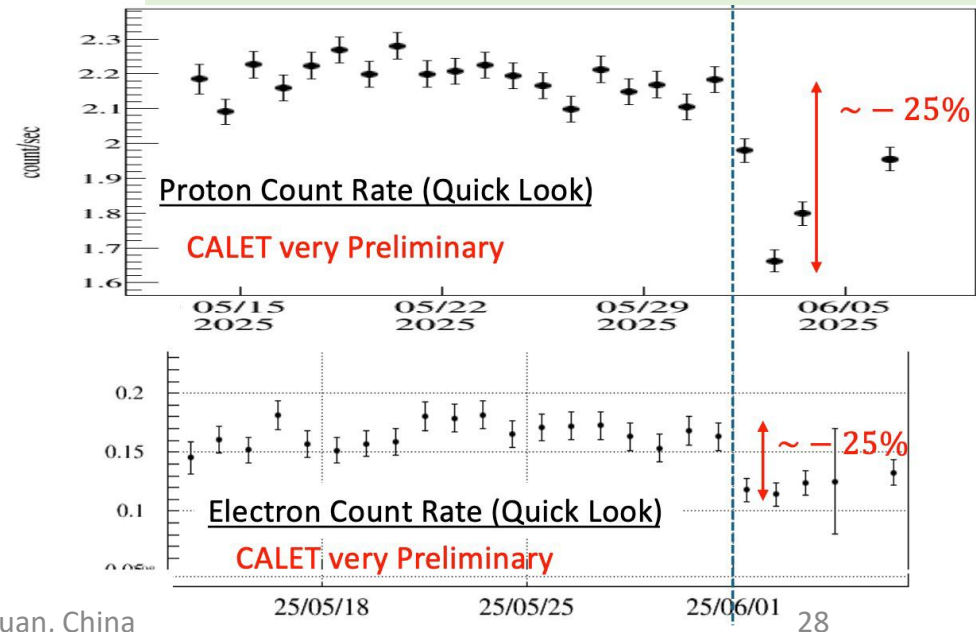
PRL 130, 211001 (2023)
ICRC 2025 Update

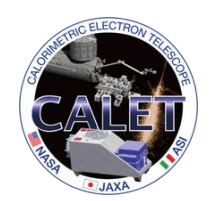
electron and proton count rates
at an average rigidity of 3.8 GV



- CALET have been recorded the count rates of proton/electron $>1\text{GeV}$ in the past 10 years including the solar minimum and the solar maximum.
- We have observed a clear charge-sign dependence of the solar modulation of galactic cosmic-rays and have succeeded in reproducing variations with a numerical drift model.

Forbush decrease observed in Jun. 2025

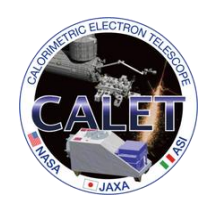




Summary

- CALET has been running stably for 10 years after the launch in Aug. 2015.
- HE trigger operation for >3368days with >86% live time.
- Total number of >GeV triggers ~5billion.
- We have achieved the following observations:
 - Cosmic-ray spectra: electron/proton/He/B/C/O/Fe/Ni/more
 - Solar modulation/diffuse and point source gamma-ray/GRB/GW follow up.
- New results:
 - Ti/Cr/Fe (PRL 135, 021002 (2025))
 - UH ($14 \leq Z \leq 44$) (APJ 988:148 (2025))
- Extended operations has been approved by JAXA/NASA/ASI through 2030.

We greatly appreciate JAXA staff for great support of the CALET operations at the TKSC of JAXA!



Backup



Overview of CALET Payload

CAL

- Charge Detector (CHD)
- Imaging Calorimeter (IMC)
- Total Absorption Calorimeter (TASC)

CGBM

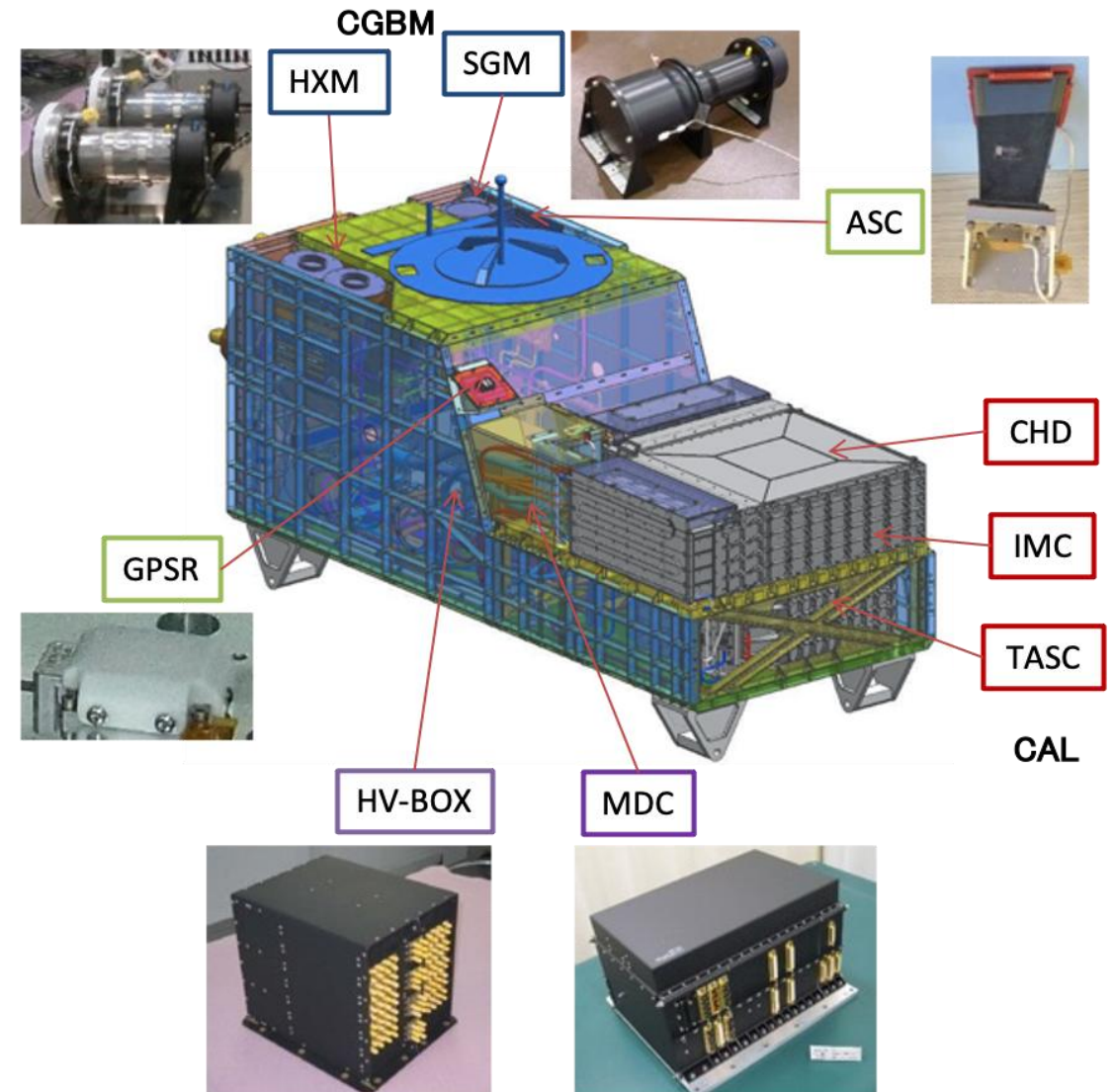
- Hard X-ray Monitor (HXM) x 2
LaBr₃ : 7keV~1MeV
- Soft γ -ray Monitor (SGM)
BGO : 100keV~20MeV

Data Processing & Power Supply

- Mission Data Controller (MDC)
CPU, telemetry, power, trigger etc.
- HV-BOX (Italian contribution)
HV supply (PMT:68ch, APD:22ch)

Support Sensors

- Advanced Stellar Compass (ASC)
Directional measurement
- GPS Receiver (GPSR)
Time stamp of triggered event (<1ms)

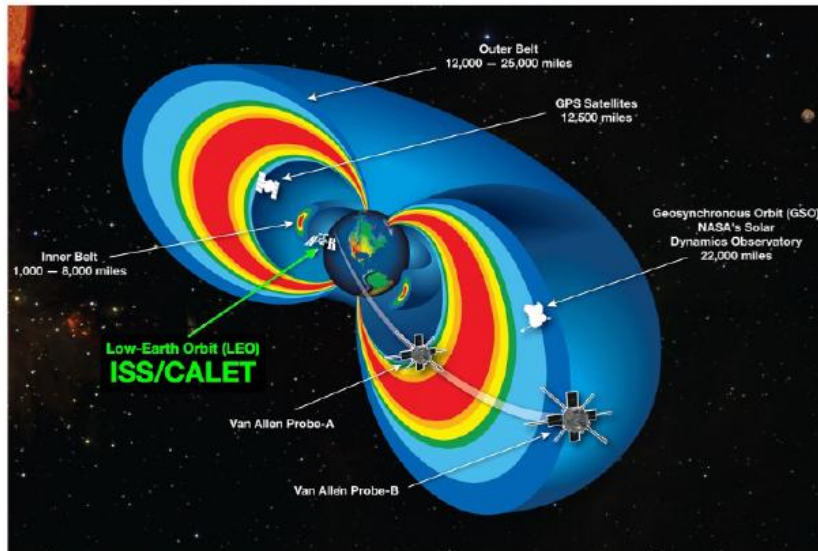




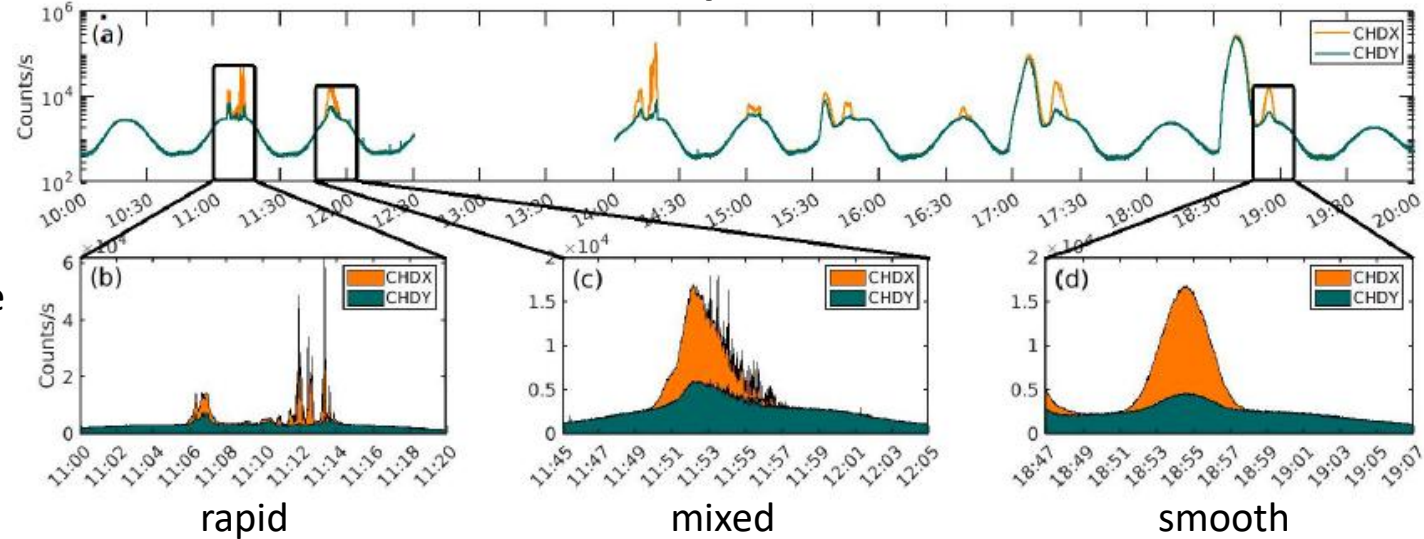
Space Weather Transients

- Objectives of CALET include continuous monitoring of space-weather phenomena in the LEO radiation environment, including relativistic electron precipitation (REP) from the outer Van Allen Belt
- REP drivers were investigated in magnetically conjugate observations by CALET and Van Allen Probes, showing the role of wave scattering and the contribution of EMIC-wave driven precipitation to radiation-belt losses (Bruno et al., 2021⁺; Blum et al., 2024⁺)

CALET and Radiation Belt Science Probes (RBSP)



Relativistic Electron Precipitation Events with CALET



- An automated algorithm based on machine-learning techniques was implemented to identify and classify the REP events collected during >9 years of the mission (Vidal-Luengo et al, 2024a^{*})
- The large statistical sample allowed to investigate the contribution of REP to the radiation belt dropouts, and the correlations with solar-wind/geomagnetic drivers (Freund et al., 2024^{*})
- The occurrence of REP events was found to exhibit a semi-annual variation (peaking at equinoxes), in agreement with the temporal periodicity of outer-belt electron intensities (Vidal-Luengo et al, 2024b⁺)